The Geological Society of America
Special Paper 548

Climate-driven late Quaternary fan surface abandonment in the NW Himalaya

Elizabeth N. Orr*
GFZ German Research Centre for Geosciences, Telegrafenberg, 14473 Potsdam, Germany, and
Institute for Geosciences, University of Potsdam, 14476 Potsdam, Germany

Lewis A. Owen*
Department of Marine, Earth, and Atmospheric Sciences, North Carolina State University, Raleigh, North Carolina 27695, USA

Sourav Saha*
Department of Earth, Planetary, and Space Sciences, University of California, Los Angeles, California 90095, USA

Marc W. Caffee*
Department of Physics, Purdue University, West Lafayette, Indiana 47907, USA, and
Department of Earth, Atmospheric and Planetary Sciences, Purdue University, West Lafayette, Indiana 47907, USA

ABSTRACT

We defined the timing of surface abandonment for 10 alluvial and debris-flow fans across contrasting climatic settings in the NW Himalaya of northern India using cosmogenic ^{10}Be surface exposure dating. Debris-flow fans in the Garhwal, Kullu, and Lahul-Spiti regions of the monsoon-influenced Greater Himalaya were largely abandoned during the Mid- to Late Holocene. Large alluvial fans and smaller debris-flow fans in the semiarid Ladakh region of the Greater and Tethyan Himalaya have surface ages that extend throughout the last glacial. Regional events of landform abandonment and incision were defined for the monsoon-influenced western Himalaya ranges and the semiarid western Himalaya ranges over the past ~120 k.y. In the monsoon-influenced and semiarid western Himalaya ranges, these regional events were limited to the Holocene and from ca. 40 ka, respectively. The timing of fan surface abandonment and regional landform abandonment events coincided with periods of weakening monsoon strength and cooling, and local and regional glacier advances. Regional incision events from the monsoon-influenced and semiarid western Himalaya regions were recognized across various climatic conditions due to the ubiquitous nature of erosion in mountain settings. This study showed that climate-driven processes and glaciation were important drivers in fan sedimentation, catchment sediment flux, and the topographic evolution of the NW Himalaya during the late Quaternary.

*E-mails: corresponding author, E.N. Orr: elizabeth.orr@gfz-potsdam.de; L.A. Owen: lewis.owen@ncsu.edu; S. Saha: sahasv@ucla.edu; M.W. Caffee: mcaffee@purdue.edu.

Orr, E.N., Owen, L.A., Saha, S., and Caffee, M.W., 2020, Climate-driven late Quaternary fan surface abandonment in the NW Himalaya, *in* Waitt, R.B., Thackray, G.D., and Gillespie, A.R., eds., Untangling the Quaternary Period: A Legacy of Stephen C. Porter: Geological Society of America Special Paper 548, https://doi.org/10.1130/2020.2548(04).

INTRODUCTION

Alluvial and/or debris-flow fans are widespread landforms throughout mountain environments. These landforms radiate from points of gradient lowering along mountain fronts and where catchments become unconfined, invariably at the mouth. In high-altitude, high-relief settings such as the Himalayan-Tibetan orogen, alluvial/debris-flow fans serve as temporary stores of poorly sorted deposits including debris-flow, glaciofluvial, fluvial, lacustrine, and eolian sediment (Ballantyne, 2002a, 2002b; Barnard et al., 2006b). Alluvial/debris-flow fans are not simply fluvial in nature; debris/mud flow, snow avalanching, and other diffusive hillslope processes also contribute to their formation (Ballantyne, 2002a; Nicholas and Quine, 2007). We refer to these landforms as "fans" in our study.

In the Himalayan-Tibetan orogen, most fans are understood to form and evolve as part of the landscape response to a shift in climate or environmental conditions (Owen and Sharma, 1998; Kumar Singh et al., 2001; Barnard et al., 2004a, 2004b, 2006a, 2006b; Srivastava et al., 2008). Studies have shown that fans frequently form as the result of enhanced catchment sediment flux following deglaciation. The climate-driven downwasting and retreat of glacier ice cause the unloading of hillslope debris, and the reworking and redistribution of glacigenic sediment to the catchment mouth. Fans in the Himalaya are found to aggrade in this way on time scales of 10^4–10^1 yr after the onset of deglaciation (Owen and Sharma, 1998; Watanabe et al., 1998; Ballantyne, 2002a).

Shifts in catchment sediment flux and the aggradation of fans can also be the result of processes and events that enhance hillslope instability. The regeneration or readvance of a glacier can exacerbate instabilities by steepening and/or debuttressing hillslopes through glacial erosion (Watanabe et al., 1998; Ballantyne, 2002a; Barnard et al., 2006b; Hewitt, 2009). Further adjustments to slope stability can occur through periglacial weathering processes, permafrost degradation, changes in runoff regime, and extreme storm and flood events (Gruber and Haeberli, 2007; Hales and Roering, 2007; Eppes and McFadden, 2008; Heimsath and McGlynn, 2008). In addition to climate, other variables that are also likely to contribute to the formation and evolution of fans include: sediment supply, source catchment lithology, seismic events, and changes to base level (Ritter et al., 1995; Pope and Wilkinson, 2005; Hobley et al., 2010; Scherler et al., 2014). Deciphering the relative roles of any one of these variables in the development of these landforms is challenging in rapidly denuding mountain settings such as the Himalaya, particularly as each factor will likely vary over space and time.

There are few quantitative studies that define the timing of fan development and stabilization in the Himalaya. Our understanding of the evolution of these landforms and the wider catchment, and the influences of climate and/or tectonism within these sedimentary systems, is therefore incomplete. Improvements in dating methods, particularly cosmogenic nuclide surface exposure dating, enable better constraints to be obtained on the age of fan surfaces (Dühnforth et al., 2007; Blisniuk et al., 2012; Cesta and Ward, 2016). Cosmogenic nuclide surface exposure ages define the timing of fan surface abandonment and a period of landform stability following its formation across time scales of 10^4–10^1 yr (Pope and Wilkinson, 2005; Owen et al., 2014).

Well-preserved fans in the NW Himalaya provide an excellent opportunity to assess the controls on fan formation in a high-relief mountain setting, as well as evaluate how these controls may vary between areas of contrasting climatic regime. Here, we report 18 new and 29 recalculated ^{10}Be fan surface ages for a suite of 10 fans across the Greater Himalaya ranges of northern India. This study focused on three new study areas: the Kullu and Chandra valleys in the monsoon-influenced Kullu and Lahul-Spiti regions in Himachal Pradesh, and the Karzok valley, located in the semiarid Ladakh region in Jammu and Kashmir (Fig. 1). We also revisited the study areas of the Tangtse valley in Ladakh, and the Bhagirathi and Gori Ganga valleys in the warm-wet Garhwal region of Uttarakhand. We compared the fan surface ages in our study with local and regional climate and glacial records to evaluate the contributions of climate and climate-driven surface processes in the timing of fan aggradation and stabilization in the NW Himalaya throughout the late Quaternary.

In this study, regional landform abandonment and incision events were defined for the monsoon-influenced Lesser and Greater Himalaya, and the semiarid interior ranges of the Greater and Tethyan Himalaya using geomorphic records throughout the NW Himalaya (Fig. 1). This record was compared to the fan surface ages to explore possible patterns or times of regional landscape change in response to climate. We also discuss the effect of preservation bias within geomorphic evidence in the understanding of landscape change throughout the NW Himalaya.

REGIONAL SETTING

The regional geologic setting of the study area is the consequence of the continued collision and partial subduction between the Indian and Eurasian continental lithospheric plates, commencing at ca. 55 Ma (Searle et al., 1986). In the NW Himalaya, the Indus-Tsangpo suture zone marks the collision zone between these continental plates and the northern boundary of the Tethyan Himalaya. Deformation-driven crustal shortening from the early Miocene to the Pleistocene initiated the development of series of foreland-propagating thrust systems that divide the Himalayan lithotectonic units south of the Tethyan Himalaya into the High Himalaya crystalline sequence, the Lesser Himalaya crystalline sequence, the sub-Himalaya, and the foreland basin (Searle, 1986; Steck et al., 1998; Schlup et al., 2003; Vannay et al., 2004; Thakur et al., 2014).

The climate in the NW Himalaya is primarily governed by the midlatitude westerlies, which bring most of the precipitation during the winter from the Mediterranean, Black, and Caspian Seas (Mölg et al., 2014), and the south Asian summer monsoon, which advects moisture from the Indian Ocean, bringing enhanced summer precipitation to the high-altitude southern frontal ranges of

the orogen (Benn and Owen, 1998, 2002; Bookhagen and Burbank, 2006, 2010; Owen, 2009). The imposing orographic barrier of the Himalaya range creates a steep precipitation gradient, perpendicular (S–N) to the strike of the mountain belt (Qiang et al., 2001; Liu and Dong, 2013). The northward decline in annual precipitation today falls from ~1500–3000 mm in the Lesser and Greater Himalaya ranges to <150 mm in the interior of the Tibetan Plateau (Tropical Rainfall Measuring Mission [TRMM] data 1998–2005 *in* Bookhagen and Burbank, 2006). Strong variability in climate throughout the late Quaternary is considered to have significantly influenced the rate and magnitude of landscape change (Prell and Kutzbach, 1987; Gasse et al., 1996; Shi et al., 2001; Bookhagen et al., 2005; Bookhagen and Burbank, 2006; Wulf et al., 2010) and nature and timing of glaciation (Owen and Dortch, 2014) in the Himalayan-Tibetan orogen.

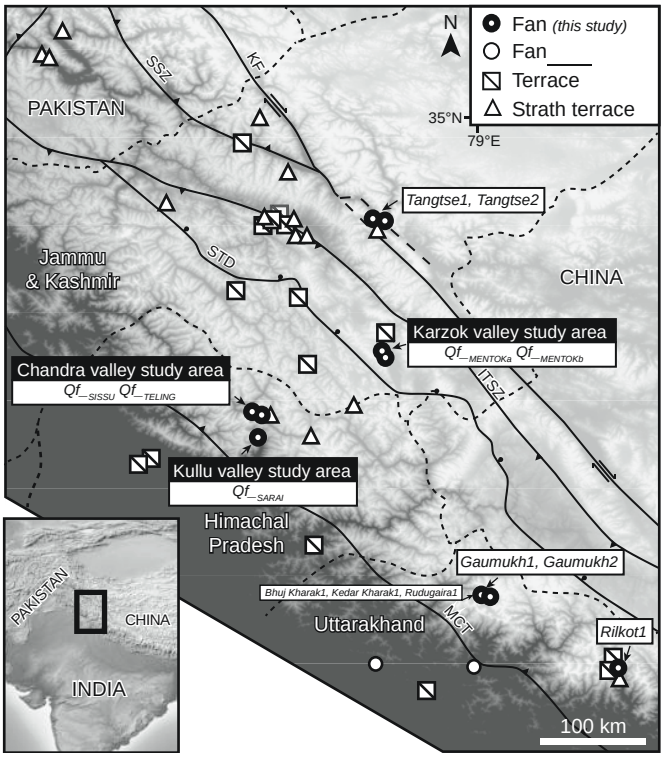

Figure 1. Location of the study areas overlying a digital elevation model. Geologic structures are from Hodges (2000): ITSZ—Indus-Tsangpo suture zone; KF—Karakoram fault; MCT—Main Central thrust; SSZ—Shyok suture zone; STD—South Tibetan detachment. Fans of this study (see Table 1 and Fig. 5 for precise locations): Gori Ganga, Nanda Devi, NE Garhwal (*Rilkot1*; Barnard et al., 2004a); upper Bhagirathi valley, Garhwal (*Bhuj Kharak1, Kedar Kharak1, Rudugaira1, Gaumukh1, Gaumukh2*; Barnard et al., 2004b); Kullu valley (Qf_{-SARAI}); Chandra valley (Qf_{-SISSU}, $Qf_{-TELING}$); Karzok valley ($Qf_{-MENTOKa}$, $Qf_{-MENTOKb}$); Tangtse valley, Ladakh (*Tangtse1, Tangtse2*; Brown et al., 2002, 2003; Dortch et al., 2011c). Fan studies are from Kumar Singh et al. (2001) and Srivastava et al. (2017). Terrace studies are from Barnard et al. (2004a, 2004b); Bookhagen et al. (2006); Dortch et al. (2011a); Blöthe et al. (2014); Scherler et al. (2015); and Dey et al. (2016). Strath terrace studies are from Burbank et al. (1996); Leland et al. (1998); Barnard et al. (2001, 2004a, 2004b); Seong et al. (2007); Adams et al. (2009); and Dortch et al. (2011a, 2011b). Inset map illustrates the location of the overall study area within the Himalayan-Tibetan orogen (base map from http://www.geomapapp.org).

There is growing contention around whether the morphostructural and landscape evolution of the mountain belt is the result of climate-topography interactions and/or underlying tectonism. Most studies argue that the spatial distribution of erosion is a function of orographically focused monsoon rainfall (Bookhagen et al., 2005; Bookhagen and Burbank, 2006; Gabet et al., 2004; Wulf et al., 2010). This relationship is not straightforward, however, because the distribution and magnitude of precipitation on the regional scale vary both spatially and temporally, and local microclimates are retained throughout individual mountain ranges. Moreover, sporadic heavy rainfall has been argued to govern the sediment flux of Himalayan catchments (Hasnain, 1996; Craddock et al., 2007; Wulf et al., 2010). The opposing view is that patterns in erosion are instead determined by structurally controlled rock uplift (Lavé and Avouac, 2001; Burbank et al., 2003; Thiede et al., 2004; Scherler et al., 2014; Orr et al., 2019).

Most Greater Himalaya glaciers today are large, temperate, and melt-dominated features, and they are fed by monsoonal precipitation (Benn and Owen, 2002; Su and Shi, 2002). Glaciers in the semiarid Greater Himalaya are usually small (1–10 km^2), cold-based, subpolar types, which are precipitation sensitive and sublimation dominated (Benn and Owen, 2002). Evidence of three to four glacial stages per catchment is typically preserved throughout the western Himalaya (Owen and Dortch, 2014). We synthesized the glacial records of the NW Himalaya using the following regional chronostratigraphies: the semiarid western Himalayan–-Tibetan orogen stages of Dortch et al. (2013), monsoonal Himalayan-Tibetan stages of Murari et al. (2014), and Himalayan Holocene stages of Saha et al. (2018, 2019). Dortch et al. (2013) and Owen and Dortch (2014) argued that the nature, timing, and forcing of glaciation vary over short distances (10^1–10^2 km) within individual mountain ranges. Broadly, glacier advances in the NW Himalaya are moderated by monsoon strength (Owen and Sharma, 1998; Watanabe et al., 1998). Our study areas were selected because the local glacial successions have been dated using cosmogenic nuclides (Table 1).

The Kullu valley study area is located on the southern slopes of the Pir Panjal Range of the Greater Himalaya in the Kullu district of Himachal Pradesh (Fig. 1; Table 1). This large transverse drainage system extends ~60 km from the source of the Solang Nala and Beas Rivers (~3400 m above sea level [asl]) to the village of Larji (~1000 m asl). The study area is limited to the upper reaches of the Kullu valley (>1700 m asl), where bajada-style fan complexes sourced from the eastern and western tributaries occupy the valley (Owen et al., 1995).

The Chandra valley is a large longitudinal drainage system in the Lahul-Spiti district of Himachal Pradesh, in the rain shadow of the Pir Panjal Range (Fig. 1; Table 1). The study area extends along the northwest-flowing Chandra River from Koksar

TABLE 1. CLIMATE AND GLACIAL RECORDS FOR THE KULLU, CHANDRA, AND KARZOK VALLEY STUDY AREAS

	Climate			Glacial record
	Mean annual precipitation (mm)	Mean annual temperature range (°C)	Vegetation	
Kullu valley study area*	2000−3000	–4 to 11	Dense broad-leaved, coniferous and subalpine forest	15.5 ± 0.5 ka (Rhotang Pass Stage), 12.2 ± 1.6−10.6 ± 0.3 ka (Solang Stage; Owen et al., 2001)
Chandra valley study area†	(a) >500 (predom. >900) (b) 400−800	(a) –12 to 6 (b) –15 to 7	Alpine herbs, sedges, grasses, and subalpine forest	15.3 ± 1.6 ka (Batal Stage; Murari et al., 2014), 12.4 ± 1.2 ka (Kulti Stage; Murari et al., 2014), 10.4 ± 0.3 ka (mH3), 0.2 ± 0.1 ka (mH1a; Saha et al., 2018) Last Glacial Maximum deglaciation: ca. 20−14 ka (Eugster et al., 2016)
Karzok valley study area§	(a) ~115 (b) 40−100	(a) –2.8 to 24.7	Xerophytic shrubs and grasses	311.0 ± 8.0 ka (KM-0), 126.0 ± 8.0 ka (PM-0), 72.0 ± 31.0 ka (KM1-3), 47.0 ± 12.0 ka (PM-1), 2.7 ± 2.3 ka (PM-2), 0.3 ± 0.2 ka (PM-3; Hedrick et al., 2011; Dortch et al., 2013) 4.9 ± 0.3 ka (KM-4/mG2), 2.1 ± 0.2 ka (mM2), 1.0 ± 0.1 ka (mM1), 0.7 ± 0.1 ka (mM1; Hedrick et al., 2011; Dortch et al., 2013; Saha et al., 2018)

*Kullu valley: Dhundi weather station (32.2530°N, 77.1299°E, 2850 m above sea level [asl]); Snow and Avalanche Establishment (SASE) 1993−2001 (Gusain et al., 2004), TRMM 1998−2005 (Bookhagen and Burbank, 2006), vegetation from Rawat et al. (2015).
†Chandra valley: (a) Chhota Shigri weather station (32.2867°N, 77.5365°E, 3900 m asl); 1980−2005 (Wagnon et al., 2007; Azam et al., 2014); (b) TRMM 1998−2005 (Bookhagen and Burbank, 2006), Patseo weather station (32.7538°N, 77.2610°E, 3780 m asl); Snow and Avalanche Establishment (SASE) 1993−2001 (Gusain et al., 2004); vegetation from Rawat et al. (2015).
§Karzok valley: (a) Leh weather station (34.1800°N, 77.5800°E, 3500 m asl); CRUTEM4 1876−1990 (Jones et al., 2012; Osborn and Jones, 2014); (b) TRMM 1998−2005 (Bookhagen and Burbank, 2006).

(32.4141°N, 77.2351°E) to Sissu (32.4805°N, 77.1220°E), and it is characterized by highly dissected fans along the valley floor.

The Karzok valley is located in the high-altitude, semiarid desert of the Zanskar Range, Ladakh region in Jammu and Kashmir (Fig. 1; Table 1). The study area is composed of a series of northeast-trending tributary catchments draining the Rupshu Massif. A broad bajada extends along the flank of the massif.

METHODOLOGY

Our investigated valleys have small glaciated and nonglaciated tributary catchments that contain a wealth of well-preserved Quaternary deposits and landforms. Fans composed of diamicts and gravels are particularly abundant in these study areas (Derbyshire and Owen, 1990; Owen et al., 1995; Barnard et al., 2004a, 2004b, 2006b).

Field Methods

Detailed geomorphic maps of each study area were made in the field aided by Landsat Enhanced Thematic Mapper Plus (ETM+) imagery (30 m resolution), topographic maps generated from Advanced Spaceborne Thermal Emission and Reflection Radiometer (ASTER) global digital elevation models (V002, 30 m resolution), and Google Earth imagery. Landforms and sediments were described and differentiated using the geomorphic and sedimentological methods and criteria of Benn and Owen (2002).

Topographic and geomorphic metrics for the study areas and investigated fans were calculated from an ASTER V002–derived digital elevation model (30 m resolution) using the Spatial Analyst toolbox in ESRI's ArcMap 10.1 (Table 1).

Fans in each study area were assigned names based on their source catchment and, where appropriate, were numbered from oldest to youngest (1 to *n*) based on their morphostratigraphic position within the catchments (Hughes et al., 2005; Hughes, 2010). As an example, $Qf_{-GOMUCHE03}$ (Qf = Quaternary fan) was located furthest downstream (subscript 03) from the Gomuche tributary catchment (subscript GOMUCHE).

The best-preserved fans with clearly defined proximal and distal zones and little evidence of surface denudation, deflation, or human modification were selected for further investigation and ^{10}Be dating. The investigated fans included: Qf_{-SARAI} from the Kullu valley; Qf_{-SISSU} and $Qf_{-TELING}$ from the Chandra valley; and $Qf_{-MENTOKa}$ and $Qf_{-MENTOKb}$ from the Karzok valley.

Three to five boulders of quartz-bearing lithologies were sampled for ^{10}Be dating on each fan surface. Approximately 500 g samples of rock with thicknesses of 1–5 cm were removed from each boulder surface using a hammer and chisel. The sampled boulders were described and photographed (Appendix S1[1]), and their locations were recorded using a handheld Garmin Etrex 30

[1]Supplemental Material. Sample details of local and regional chronological datasets. Please visit https://doi.org/10.1130/SPE.S.12174543 to access the supplemental material, and contact editing@geosociety.org with any questions.

global positioning system unit. Topographic shielding was measured at 10° azimuths from the boulder surface to the horizon using a compass and inclinometer.

Large tabular boulders with varnish and/or lichen cover, well set into the fan surface, were preferentially selected for sampling; sampling large boulders reduces the likelihood of selecting ones that have recently toppled or been exhumed (Benn and Owen, 2002; Heyman et al., 2011). Boulders were avoided if there was evidence of strong weathering, pitting, fracturing, exfoliation, or shielding from regolith. Likewise, boulders adjacent to or within areas with evidence of human modification of the landscape were not sampled. Boulders were only sampled from the distal zones of each fan to restrict the likelihood of them being derived from adjacent slopes through rockfalls. Boulders in ephemeral channels were also avoided.

The ^{10}Be age of each fan surface was defined by the range of boulder exposure ages. The age range defines the timing of the abandonment of the fan surface and cessation of fan aggradation (Pope and Wilkinson, 2005; Owen et al., 2014; Cesta and Ward, 2016). A broad range of ^{10}Be ages may be the result of inheritance, boulder weathering, toppling, or shielding, or it may indicate that multiple sedimentation events characterize the fan surface (Zehfuss et al., 2001; Blisniuk et al., 2012; Hedrick et al., 2013). No statistical treatment of the ^{10}Be ages was possible due to the restricted size of the data set and distribution of ages for each landform.

Laboratory Methods

Crushing and sieving of the rock samples, quartz isolation, dissolution, chromatography, isolation of Be, and the preparation of BeO were performed at the Geochronology Laboratories at the University of Cincinnati, using the chemical procedures and community standards of Kohl and Nishiizumi (1992) and Nishiizumi et al. (1994), modified by Dortch et al. (2009). The isolated BeO was mounted onto steel cathodes, and the ^{10}Be/^{9}Be sample ratios were measured using accelerator mass spectrometry (AMS) at the Purdue Rare Isotope Measurement Laboratories (PRIME) at Purdue University (Sharma et al., 2000).

^{10}Be Fan Exposure Ages

The ^{10}Be boulder exposure ages were calculated using the Cosmic Ray Exposure program calculator (CREp) of Martin et al. (2017), using the LSD scaling model (Lifton et al., 2014) with the ERA40 atmospheric model (Uppala et al., 2005) and Lifton VDM 2016 geomagnetic database. This calculation scheme accounts for nuclide-specific production rate sensitivities to temporal and spatial variability in geomagnetic and solar inputs (Lifton et al., 2014), and it has been successfully applied throughout the NW Himalaya, particularly for the Holocene (Orr et al., 2018; Saha et al., 2018). Published ^{10}Be ages of the revisited Garhwal (Barnard et al., 2004a, 2004b) and Ladakh (Brown et al., 2002, 2003; Dortch et al., 2011c) fans were recalculated using these same methods, to allow for comparisons between fan records. The exposure ages were calculated assuming zero erosion. The effect of erosion is considered negligible owing to the very low 0.5–2.3 m/m.y. rates measured throughout the Ladakh Range of northern India (Dortch et al., 2011b; Dietsch et al., 2015).

Regional Landform Abandonment and Incision Events in the NW Himalaya

Probability density functions of phases of landform abandonment and incision for the monsoon-influenced Lesser and Greater Himalaya ranges and semiarid interior ranges of the Greater Himalaya and Tethyan Himalaya were defined by numerically dated river terrace, strath terrace, and fan surfaces from existing geomorphic studies (Fig. 1). Previously published numerical cosmogenic ages were recalculated using the same calculation scheme as was used for our new fan ages (Appendices S3 and S4). The monsoon-influenced western Himalaya region includes the Lahul-Spiti, Kullu, Simla, Uttarkashi, and Garhwal Districts of northern India, while semiarid western Himalaya ranges span the Ladakh region of northern India and the Karakoram ranges of northeastern Pakistan. Regional events in landform abandonment and incision were defined by ≥3 ages. Landform abandonment events refer to times of restricted sedimentation during which landforms stabilize.

LANDFORM DESCRIPTIONS

The Qf_{-SARAI} (32.3095°N, 77.1568°E) fan in the Kullu valley study area is sourced from the Sarai tributary—a steep-relief, unglaciated catchment with a parallel drainage system. The fan is located at the confluence between the Solang Nala and Beas Rivers at ~2300 m asl (Tables 2 and 3; Fig. 2). The source catchment of the Qf_{-SISSU} fan (32.4827°N, 77.1176°E) in the Chandra valley study area is located adjacent to the Sissu Nala catchment (Figs. 3A–3C). This steep-relief catchment has preserved evidence of past glaciation, but it is presently not glaciated. $Qf_{-TELING}$ (32.4357°N, 77.1926°E) is sourced from the Teling tributary, ~6 km northwest from Koksar (Figs. 3D–3F). This glaciated amphitheater preserves an abundance of landforms and sediment deposits including moraines, talus, and mass movements. In the Karzok valley study area, $Qf_{-MENTOKa}$ (32.9647°N, 78.2381°E) represents the most easterly fan of the bajada, sourced from a Mentok catchment that has a cirque glacier. Similar morphology is shared by the second Mentok tributary catchment located directly adjacent to, and to the northwest of, the first—the source catchment for $Qf_{-MENTOKb}$ (32.9701°N, 78.2301°E; Tables 2 and 3; Fig. 4).

RESULTS

New and Recalculated Fan Surface ^{10}Be Ages

Fan surfaces in the Kullu and Chandra valley study areas have ^{10}Be boulder ages younger than 12 ka, with the majority younger than 4 ka. The ^{10}Be ages for the Karzok valley fan

TABLE 2. SOURCE CATCHMENT AND FAN METRICS FOR THE KULLU, CHANDRA, AND KARZOK VALLEY STUDY AREAS

	Catchment characteristics						Fan characteristics						
Fan no.	Headwall (m asl)	Area (km²)	Aspect (°)	Relative Relief* (m)	Mean slope† (°)	HI index§	Channel profile (°)	Apex (m asl)	Area (km²)	Aspect (°)	Mean slope (°)	Mean channel depth# (m)	Mean channel width# (m)
Kullu valley													
Qf_{-SARAI}	5060	18.8	90	250	35	0.4	15	2510	1.5	115	8	0.7	48.3
Chandra valley													
Qf_{-SISSU}	5730	12.2	205	195	30	0.5	18	3210	0.7	225	15	10.8	13.8
$Qf_{-TELING}$	5710	17.9	205	250	35	0.6	16	3190	0.5	205	11	3.1	18.3
Karzok valley													
$Qf_{-MENTOKa}$	6200	17.8	45	130	18	0.5	10	4880	1.9	20	8	2.3	5.9
$Qf_{-MENTOKb}$	6090	17.1	45	130	19	0.5	10	4790	1.2	45	6	2	5.1

*Mean relative relief was derived from 0.13 km² catchment grid cells. Catchment relative relief (m): Qf_{-SARAI} (2276); Qf_{-SISSU} (2772); $Qf_{-TELING}$ (2619); $Qf_{-MENTOKa}$ (1642); $Qf_{-MENTOKb}$ (1520).
†Slope derived from 0.001 km² catchment grid cells.
§Strahler (1952) hypsometric index (HI = mean elevation – minimum elevation/relief).
#Mean depth and width derived from 10 channel cross-section profiles between apex and distal zone of fan.

surfaces range between ca. 110 and 12 ka (Fig. 5; Table 4; Appendix S1).

The Kullu valley Qf_{-SARAI} fan surface has ^{10}Be ages between 7.8 ± 1.1 and 2.8 ± 0.2 ka (uncertainties for all ages are quoted to 1σ). The Qf_{-SISSU} and $Qf_{-TELING}$ fan surfaces in the Chandra valley study area have ^{10}Be age ranges of 10.9 ± 0.6–2.4 ± 0.3 ka and 11.8 ± 1.6–0.6 ± 0.1 ka, respectively. In the Karzok valley study area, $Qf_{-MENTOKa}$ has ^{10}Be ages between 110.8 ± 2.2 and 64.5 ± 0.5 ka, while the $Qf_{-MENTOKb}$ *fan* surface has ages from 66.1 ± 1.3 to 12.6 ± 0.3 ka. No ages were discounted from the data set because the restricted number and distribution of ^{10}Be ages for each landform prevented the identification of age outliers.

The recalculated ages for the *Rilkot1* fan surface in the Gori Ganga valley, northeast Garhwal range from 1.8 ± 0.2 to 0.9 ± 0.1 ka (Appendix S2 [see footnote 1]). In the Bhagirathi valley, *Gaumukh1* and *Gaumukh2* fan surfaces have ^{10}Be ages that range from 5.5 ± 0.2 to 3.1 ± 0.2 ka and from 1.5 ± 0.3 to 1.2 ± 0.2 ka, respectively. Additional fan surfaces with only one exposure age were also recalculated for this valley (*Bhuj Kharak1*: 3.27 ± 0.47 ka; *Kedar Kharak1*: 9.8 ± 0.6 ka; *Rudugaira1*: 7.8 ± 0.5 ka), but they are not discussed herein. The surface ages for the northern Ladakh *Tangtse1* and *Tangtse2* fan surfaces range from 38.6 ± 2.6 to 19.0 ± 1.5 ka and from 14.3 ± 1.5 to 2.1 ± 0.2 ka, respectively.

Regional Landform Abandonment and Incision Events for the NW Himalaya

Records of landform abandonment were recognized in the monsoon-influenced western Himalaya ranges region throughout the past ~50 k.y., with regional events at 1.4 ± 0.5 and 0.6 ± 0.2 ka (Fig. 6; Appendices S3 and S4 [see footnote 1]). Records of incision extend from ca. 70 to 0.6 ka, with regional incision events at 6.9 ± 3.7, 3.6 ± 1.0, 1.8 ± 0.6, and 1.0 ± 0.1 ka. In the semiarid western Himalaya ranges region of the NW Himalaya, records of landform abandonment extend over the past 56 k.y. and >110 k.y. Regional events occurred at 31.5 ± 5.1 ka and 20.0 ± 5.3 ka. Records of incision are recognized throughout the past ~120 k.y., with regional events occurring at 35.9 ± 5.8, 13.7 ± 3.9, and 2.2 ± 1.7 ka.

DISCUSSION

The *Rilkot1* (1.8 ± 0.2–0.9 ± 0.1 ka), *Gaumukh1* (5.5 ± 0.3–3.1 ± 0.3 ka), and *Gaumukh2* (1.5 ± 0.3–1.2 ± 0.3 ka) debris-flow fans in Garhwal have fan surfaces dating to the Mid- to Late Holocene, at a time of increasing aridity and relative cooling (Fig. 6; Gasse et al., 1996; Fleitmann et al., 2003, 2007; Dykoski et al., 2005; Wang et al., 2005; Herzschuh, 2006; Hu et al., 2008; Dong et al., 2010; Leipe et al., 2014; Rawat et al., 2015; Hudson et al., 2016; Srivastava et al., 2017). These conditions resulted from a decline in monsoon intensity and the strengthening of the midlatitude westerlies due to cooling in the North Atlantic (Clift et al., 2012; Leipe et al., 2014). Local glacial stages were recognized ~1–2 k.y. before the stabilization and abandonment of these surfaces; *Rilkot1* postdates the m_2 stage (4.4 ± 0.1–1.9 ± 0.3 ka), and *Gaumukh1* and *Gaumukh2* follow the Shivling (ca. 5.2 ka) and Gangotri (ca. 2.4–1.9 ka) stages, respectively (Sharma and Owen, 1996; Barnard et al., 2004b; Srivastava, 2012). Srivastava et al. (2017) argued that the prevailing cold and dry conditions were punctuated by short-term warm-wet periods between ca. 5.4 and 3.8 ka. The Garhwal fans therefore likely evolved during these periods of glacial advance or enhanced temperature and precipitation before being abandoned thereafter.

The Qf_{-SARAI} debris-flow fan surface (7.8 ± 1.2–2.8 ± 0.3 ka) in the Kullu valley was also abandoned during this period of increasing aridity and relative cooling in the Mid- to Late Holocene (as referenced above). Although no local glacial stages

TABLE 3. FAN AND SURFACE BOULDER DESCRIPTIONS FOR THE KULLU, CHANDRA, AND KARZOK STUDY AREAS

Fan no.	Landform description	Surface boulder description
Kullu valley		
Qf_{-SARAI}	• Slightly weathered, matrix (sand)–supported, bouldery gravel diamicton. • No morphostratigraphically younger units or sublobes on surface. Overlies older fan at Palchan (Fig. 2A). • Solang Nala and Beas River truncate northern margins of mid- and distal zones. • Sarai Nala incises into fan revealing cut banks and terraces. • Shallow, sinuous ephemeral and/or abandoned channels across fan surface. • Montane forests and grasslands, well-developed soils for agricultural land use. • Human settlement and infrastructure across fan surface.	• Distributed across northern extent of fan. Anthropogenic boulder clearing evident on southern flank. • Granitic, subangular-subrounded boulders (≤10 m; Figs. 2B and 2C). • Tabular, well-set boulders with no landform degradation/erosion at boulder margins. • Slightly to moderately weathered (minor exfoliation). Rock varnish and lichen present.
Chandra valley		
Qf_{-SISSU}	• Slightly to moderately weathered, bouldery gravel diamicton with sandy-silt matrix. • Overlies a morphostratigraphically older fan at Sissu. • Small sublobe extends from the distal region of fan at tributary-river confluence. • Chandra River and tributaries have incised, entrenched, and truncated the eastern extent of fan. • Alpine tundra, developed soils for agricultural land use. • Human settlement and infrastructure (including irrigation) across fan surface (Fig. 3A).	• Distributed across mid- and distal zones of fan. • Angular-subrounded granites and siltstones (≤10 m). • Tabular, well-set boulders with no landform degradation/erosion at boulder margins (Figs. 3B and 3C). • Slight-moderate weathering (minor exfoliation). Rock varnish and lichen present.
$Qf_{-TELING}$	• Slightly to moderately weathered, bouldery gravel diamicton with sandy-silt matrix. • Increased surface degradation on the western fan flank. • No morphostratigraphically younger units or sublobes on surface. • Teling Nala and Chandra River have incised and truncated the fan. • Alpine tundra, developed soils for agricultural land use. • Human settlement and infrastructure.	• Distributed across mid- and distal zones of fan. • Granitic angular-subrounded boulders (≤10 m). • Tabular, well-set boulders with no landform degradation/erosion at boulder margins (Fig. 3F). • Slight-moderate weathering (minor exfoliation). Rock varnish and lichen present.
Karzok valley		
$Qf_{-MENTOKa}$	• Surface characterized by two depositional units (upper, lower) with consistent descriptions. • Moderately to highly weathered, matrix (sandy-silt)–supported, sandy gravel diamicton with boulders. • Northeastern distal flank of fan underlies $Qf_{-MENTOKb}$. No morphostratigraphically younger units or sublobes identified on fan surface (Fig. 4A). • Distal zone truncated by the Karzok River. • Sinuous tributary transforms into a large braided system across fan surface. Channels are shallow, ephemeral, and/or abandoned. • Alpine tundra including xerophytic shrubs and grasses. Poor soil development.	• Distributed across mid- and distal zones of fan. Boulder ridges trend down-fan at channel margins. • Granitic subangular-subrounded boulders (≤3 m). • Tabular, well-set boulders with some landform degradation/erosion at boulder margins (Fig. 4D). • Moderately to highly weathered (cavernous weathering, pitting, and exfoliation). Rock varnish present.
$Qf_{-MENTOKb}$	• Surface characterized by two depositional units (upper, lower) with consistent descriptions. • Moderately to highly weathered, matrix (sandy-silt)–supported, sandy gravel diamicton with boulders. • No morphostratigraphically younger units or sublobes identified on fan surface (Fig. 4A). • Distal zone truncated by the Karzok River. • Sinuous tributary transforms into a large braided system across fan surface. Channels are shallow, ephemeral, and/or abandoned (Fig. 4B). • Alpine tundra including xerophytic shrubs and grasses. Poor soil development. • Nomadic human settlement at distal zone of fan.	• Distributed across mid- and distal zones of fan (anthropogenic boulder clearing evident in lower distal zone). Boulder ridges trend down-fan at channel margins. • Granitic subangular-subrounded boulders (≤3 m). • Tabular, well-set boulders with some landform degradation/erosion at boulder margins (Fig. 4E). • Moderately to highly weathered (cavernous weathering, pitting, and exfoliation). Rock varnish present.

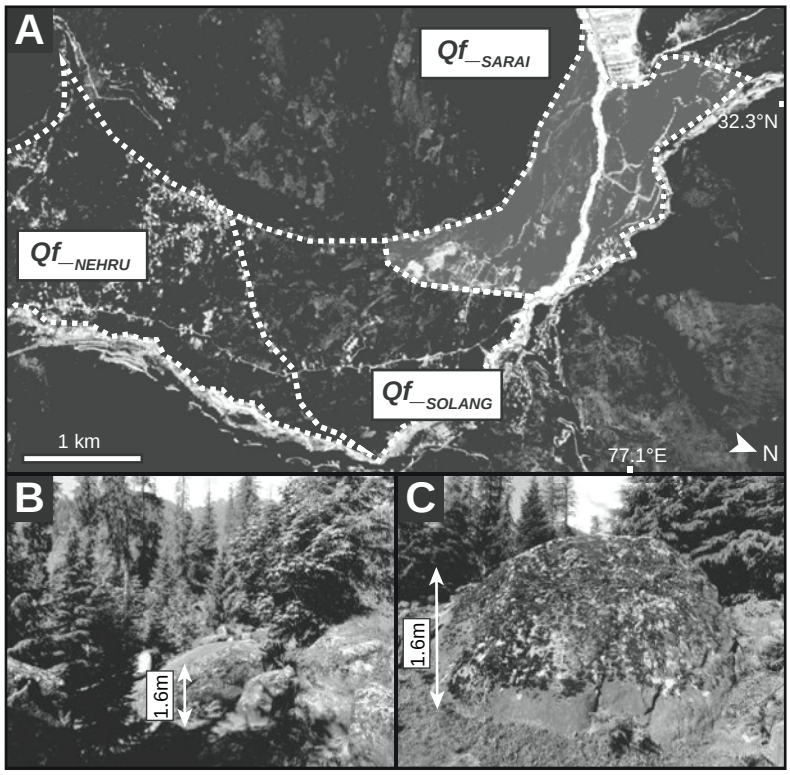

Figure 2. Kullu valley fans and typical sampled boulders. (A) Google Earth image of the Kullu valley (along Beas River from 2460 to 2030 m above sea level). $Qf_{-SOLANG}$ underlies Qf_{-SARAI} and is sourced from the Sarai and/or Solang valleys. The Nehru Kund natural spring is located at the Qf_{-NEHRU} fan (white dashed lines denote fan margins). (B) View facing east down the fan. (C) Lichen-covered sampled boulder Sar_F03.

have been recognized south of Pir Panjal at this time, the Sarai source catchment preserves a succession of moraines from past glacial advances (Owen et al., 2001). Studies have shown that an enhancement in the strength of the monsoon during the late glacial and Early Holocene caused glaciers to advance along the southern Himalayan front (Owen et al., 2001; Bookhagen et al., 2005; Saha et al., 2018). The evolution of Qf_{-SARAI} was likely, in part, affected by this glaciation.

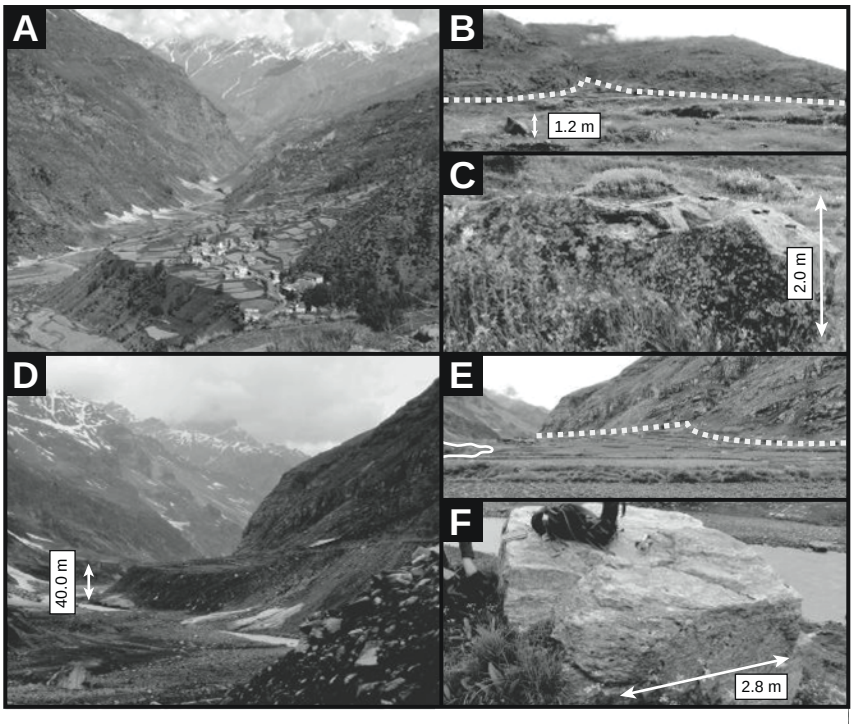

Figure 3. Fans in the Chandra valley and examples of typical boulders that were sampled for ^{10}Be dating. (A) View facing west toward Qf_{-SISSU}. (B) Image of the Qf_{-SISSU} fan apex, extent (white dashed lines), and surface. (C) Sampled boulder Sis_F03. (D) View facing west of the $Qf_{-TELING}$ fan. (E) $Qf_{-TELING}$ apex and fan surface (white dashed and solid lines denote fan perimeter and distal toe of the fan, respectively). (F) Sampled boulder Tel_F07.

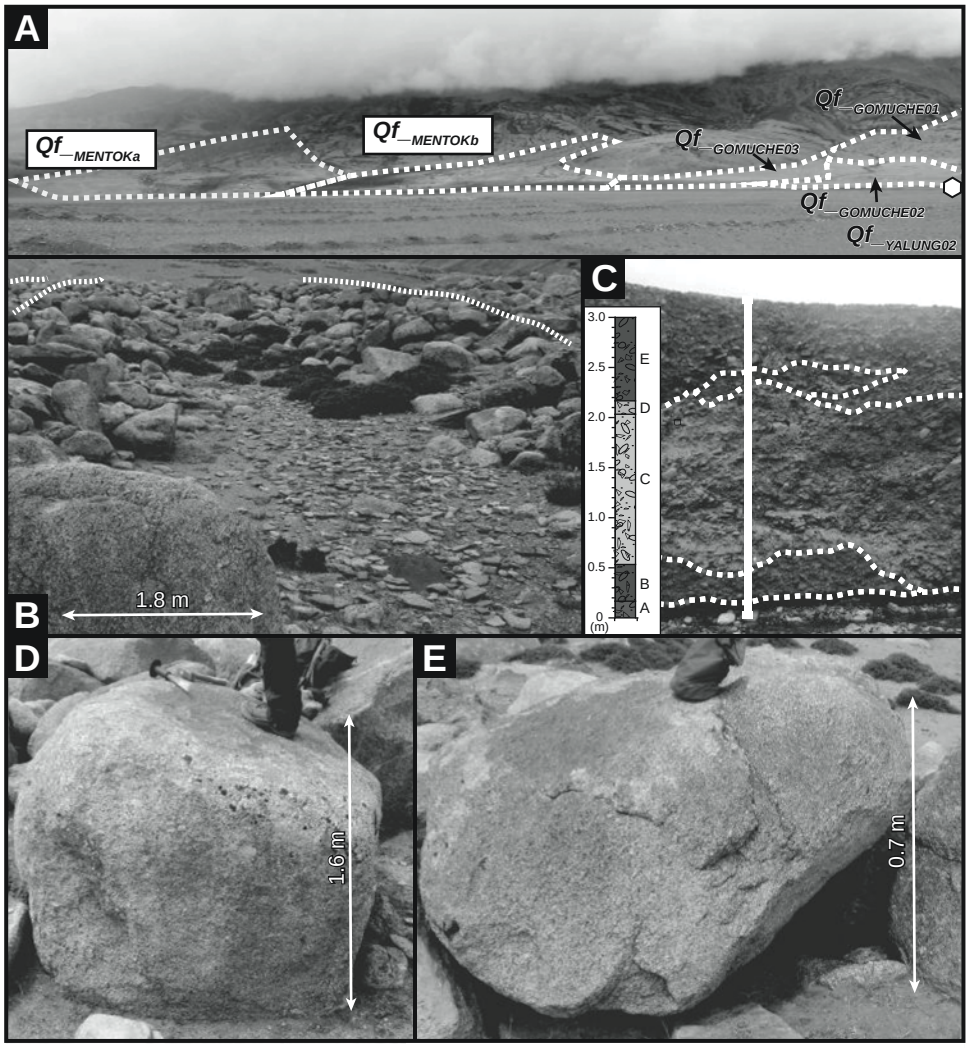

Figure 4. Views of the Karzok valley and typical sampled boulders. (A) View facing east of the Karzok valley from $Qf_{–YALUNG02}$. Dashed white lines delineate the fan extents. (B) View of boulder ridges (dashed white lines) and abandoned channels on $Qf_{–MENTOKb}$ surface. (C) Stream cut revealing multiple units of diamict upstream from the studied fans, with inset stratigraphic log (units labeled to E, from base to the surface). White dashed lines delineate the unit boundaries. Refer to A for location (white pentagon). (D) Sampled boulder Men_F03 from $Qf_{–MENTOKa}$. (E) Sampled boulder Men_F06 from $Qf_{–MENTOKb}$.

The spread in ^{10}Be ages for the $Qf_{–SARAI}$ fan is likely the result of inheritance, which is a particular problem when dating young fan surfaces and/or those composed of older reworked sediment (Gosse et al., 2003; Wittmann and Von Blanckenburg, 2009; Owen et al., 2011; Blisniuk et al., 2012; Hedrick et al., 2013). Boulder weathering, exhumation, toppling, and shielding by sediment, snow, or ice also affect the ^{10}Be inventory of a boulder surface, producing exposure ages younger than the timing of its emplacement on the landform's surface. These geological factors and other postdepositional landform disturbances by slope processes, fluvial reworking, or anthropogenic activity can produce a distribution of ^{10}Be ages on an individual fan surface.

The $Qf_{–SISSU}$ (10.9 ± 0.8–2.4 ± 0.3 ka) and $Qf_{–TELING}$ (11.8 ± 1.7–0.6 ± 0.1 ka) debris-flow fans in the Chandra valley have a broad range of fan surface ages from the Early to Late Holocene (Fig. 6). During the Last Glacial Maximum (LGM: 24–18 ka; Mix et al., 2001), a large ~200-km-long, 400–600-m-thick glacier occupied the Chandra valley and tributaries. Deglaciation of the valley extended from ca. 19 to 16 ka (Eugster et al., 2016). $Qf_{–SISSU}$ and $Qf_{–TELING}$ formed after this glacier retreat; the older ^{10}Be ages ($Qf_{–SISSU}$: 10.9 ± 0.8 ka; $Qf_{–TELING}$: 11.8 ± 1.7 ka) likely contain inheritance from the LGM. The remaining Late Holocene ages indicate that the fans were abandoned during the continued decline in relative temperatures and humidity throughout the epoch. The Teling catchment is glaciated in the present day, but both catchments retain evidence of past glacial advances. The Chandra valley fans likely formed and/or evolved in response to local glaciation.

The broad distribution of ^{10}Be ages for the Karzok valley alluvial fans ($Qf_{–MENTOKa}$: 110.8 ± 5.5–64.5 ± 2.9 ka; $Qf_{–MENTOKb}$: 66.1 ± 3.6–12.6 ± 0.7 ka) might reflect either single or multiple phases of fan surface stabilization and abandonment during the late Pleistocene (Fig. 6). We argue that the landforms were abandoned during single events and that the range in ^{10}Be ages is the result of inheritance, due to the lack of an exposure age gradient evident across the fan surfaces. Local geomorphic studies

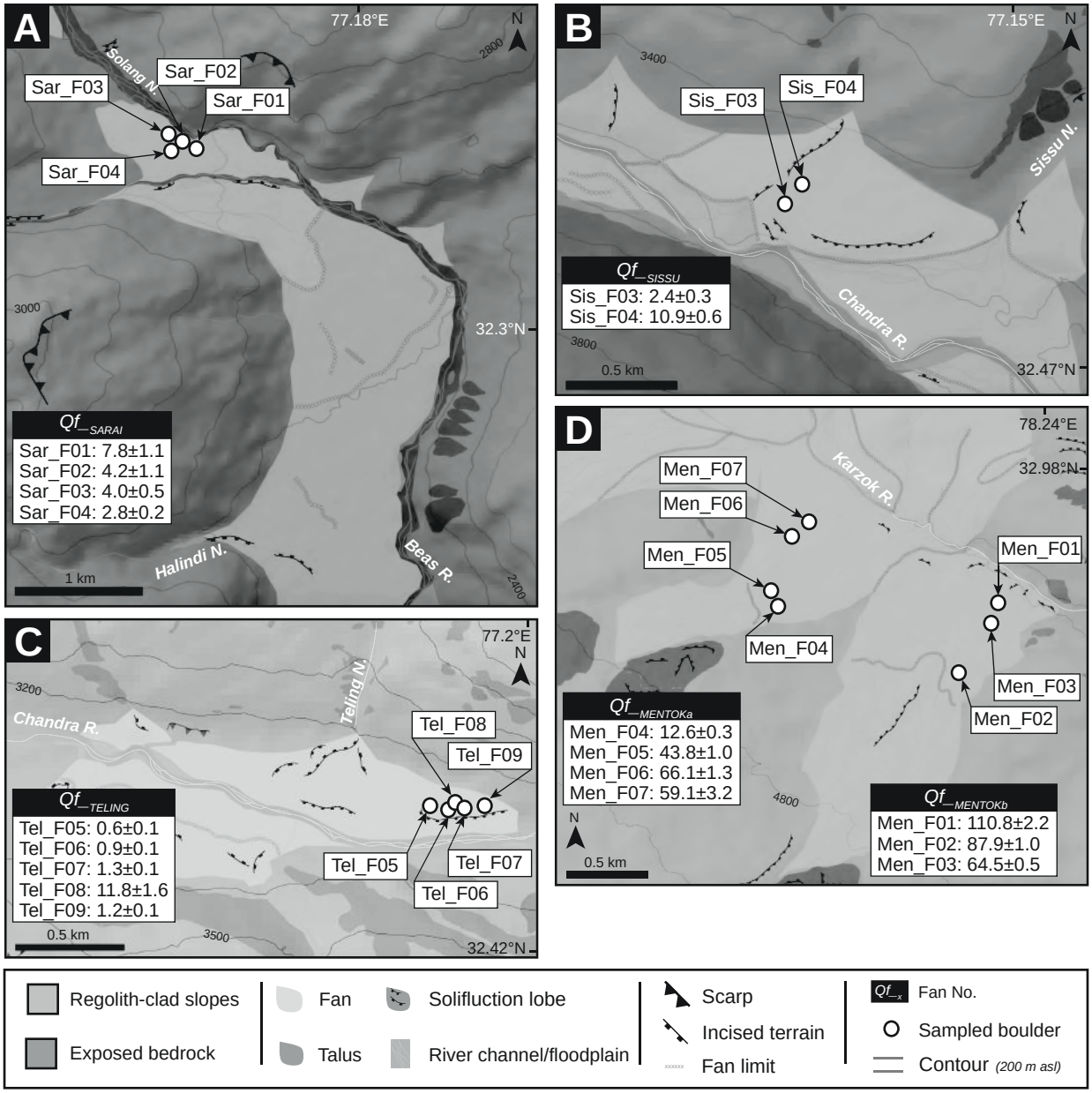

Figure 5. Geomorphology of the fan study areas showing the ^{10}Be sampling sites and ages (ka). See Figure 3 for location of each map. (A) $Qf_{–SARAI}$ study area (includes the fan and surrounding features). (B) $Qf_{–SISSU}$ study area. (C) $Qf_{–TELING}$ study area. (D) $Qf_{–MENTOKa}$ and $Qf_{–MENTOKb}$ study area. N.—Nala (stream); R.—River.

confirm that geological materials may contain inherited ^{10}Be due to the preservation of old landforms and sediment, and low rates of landscape change in the semiarid western Himalaya (Hedrick et al., 2011; Dortch et al., 2011b; Orr et al., 2017, 2018). The stable position and lack of weathering features for the Men_F04 boulder suggest that the young 12.6 ± 0.7 ka age for $Qf_{–MENTOKb}$ is due to the recent exhumation of the boulder. The timing of Karzok fan abandonment extends across times of fluctuating climatic conditions (Fig. 6). Several local glacial stages, including $Kar_{–M1}$ (132.5 ± 36.8 ka; Saha et al., 2018) and KM1–3 (72.0 ± 31.0 ka; Hedrick et al., 2011; Dortch et al., 2013), may have contributed to the formation of this extensive bajada; however, the causes of fan stabilization and abandonment remain unclear.

The *Tangtse1* debris-flow fan formed after the most recent glaciation of the Tangtse valley at 35.8 ± 3.0 ka (Fig. 6; Brown et al., 2002, 2003; Dortch et al., 2011c). The fan surface ages have a bimodal distribution; the older ages (45.1 ± 4.7–32.2 ± 2.6 ka) are likely the result of inheritance from this previous period of glaciation, or earlier. The remaining exposure ages are similar in age to the local Ladakh 2 glacial stage (22.9 ± 0.7 ka; Dortch et

TABLE 4. SAMPLE DETAILS AND ^{10}Be AGES (UNCERTAINTY IS EXPRESSED AS 1σ) FOR THE FANS OF THE STUDY AREAS

Sample name	Fan	Location		Altitude (m asl)	Boulder size			Lithology*	Weathering†	ST§ (cm)	TSF#	Quartz mass (g)	^{9}Be carrier mass, conc. (g, mg/g)	^{10}Be/^{9}Be AMS ratio** (10^{-14})	^{10}Be conc. (10^{6} atoms/g)	LSD age ± 1σ int. (ext.)†† (ka)
		Latitude (°N)	Longitude (°E)		Length (m)	Width (m)	Height (m)									
Kullu valley																
Sar_F01	Qf_{SARAI}	32.3138	77.1618	2440	3.9	2.5	1.6	L. granite	SW/MB	1	0.94	26.59	0.3501, 1.0038	14.10 ± 2.03	0.13 ± 0.02	7.8 ± 1.1 (1.2)
Sar_F02	Qf_{SARAI}	32.3138	77.1612	2453	7.7	7.2	0.8	L. granite	SW/DB	1	0.95	11.18	0.3503, 1.0038	2.91 ± 0.81	0.06 ± 0.02	4.2 ± 1.1 (1.1)
Sar_F03	Qf_{SARAI}	32.3136	77.1610	2463	4.9	3.0	1.6	L. granite	SW/MB	3	0.96	15.11	0.3503, 1.0038	3.74 ± 0.50	0.06 ± 0.008	4.0 ± 0.5 (0.5)
Sar_F05	Qf_{SARAI}	32.3136	77.1620	2437	6.4	4.0	2.3	L. granite	SW-MW/DB	2	0.95	15.40	0.349, 1.0038	2.60 ± 0.19	0.04 ± 0.003	2.8 ± 0.2 (0.3)
Chandra valley																
Sis_F03	Qf_{SISSU}	32.4808	77.1163	3100	6.0	1.5	2.0	Siltstone	SW/DB	2	0.91	3.69	0.3512, 1.0038	0.78 ± 0.09	0.05 ± 0.005	2.4 ± 0.3 (0.3)
Sis_F04	Qf_{SISSU}	32.4806	77.1161	3095	3.4	2.0	1.3	Siltstone	SW/MB	2	0.91	1.40	0.3493, 1.0038	1.51 ± 0.11	0.25 ± 0.02	10.9 ± 0.6 (0.8)
Tel_F05	Qf_{TELING}	32.4326	77.1960	3132	3.9	0.3	1.5	L. granite	SW/DB	2	0.91	19.27	0.3492, 1.0038	1.11 ± 0.11	0.01 ± 0.001	0.6 ± 0.1 (0.1)
Tel_F06	Qf_{TELING}	32.4326	77.1969	3133	9.0	2.5	2.5	L. granite	SW-MW/DB	2	0.92	15.24	0.3504, 1.0038	1.28 ± 0.18	0.02 ± 0.003	0.9 ± 0.1 (0.1)
Tel_F07	Qf_{TELING}	32.4326	77.1972	3128	4.1	2.8	0.7	L. granite	SW/MB	1	0.91	21.59	0.3492, 1.0038	2.65 ± 0.17	0.03 ± 0.002	1.3 ± 0.1 (0.1)
Tel_F08	Qf_{TELING}	32.4328	77.1970	3136	5.7	2.5	2.0	L. granite	SW-MW/MB	2	0.91	9.89	0.3495, 1.0038	12.10 ± 1.85	0.29 ± 0.04	11.8 ± 1.6 (1.7)
Tel_F09	Qf_{TELING}	32.4328	77.1981	3137	4.7	4.0	1.5	L. granite	SW/DB	2	0.92	16.35	0.3501, 1.0038	1.93 ± 0.13	0.03 ± 0.002	1.2 ± 0.1 (0.1)
Karzok valley																
Men_F01	$Qf_{MENTOKa}$	32.9679	78.2420	4633	4.5	3.0	0.7	Granite	MW/MB	1	1.00	29.88	0.3499, 1.0232	1020.00 ± 24.40	8.14 ± 0.19	110.8 ± 2.2 (5.5)
Men_F02	$Qf_{MENTOKa}$	32.9638	78.2400	4664	1.6	0.9	1.0	Granite	MW/DB	2	0.99	20.67	0.3506, 1.0038	541.00 ± 6.55	6.16 ± 0.07	87.9 ± 1.0 (4.7)
Men_F03	$Qf_{MENTOKa}$	32.9669	78.2417	4639	1.8	1.3	1.6	Granite	SW-MW/DB	2	0.99	22.21	0.3487, 1.0038	428.00 ± 6.55	4.51 ± 0.05	64.5 ± 0.5 (2.9)
Men_F04	$Qf_{MENTOKb}$	32.9680	78.2294	4673	1.5	1.0	1.7	P. granite	MW-HW/MB	2	0.98	16.35	0.3500, 1.0038	54.50 ± 1.26	0.78 ± 0.02	12.6 ± 0.3 (0.7)
Men_F05	$Qf_{MENTOKb}$	32.9687	78.2289	4673	1.4	1.1	0.9	P. granite	SW/MB	2	1.00	21.77	0.3504, 1.0800	283.00 ± 6.4	3.28 ± 0.07	43.8 ± 1.0 (2.8)
Men_F06	$Qf_{MENTOKb}$	32.9707	78.2303	4656	1.5	0.7	0.7	Granite	MW/DB	2	1.00	25.35	0.3490, 1.0038	513.00 ± 11.20	4.74 ± 0.10	66.1 ± 1.3 (3.6)
Men_F07	$Qf_{MENTOKb}$	32.9708	78.2306	4650	2.1	1.4	0.8	Granite	MW/MB	2	1.00	9.67	0.3490, 1.0038	169.00 ± 2.73	4.10 ± 0.07	59.1 ± 0.9 (3.2)

*Lithology: L. granite—leucogranite, P. granite—porphyritic granite.

†Boulder weathering characteristics: SW—slightly weathered (no pitting), MW—moderately weathered (some pitting, moderate exfoliation), HW—highly weathered (exfoliated sheets can be manually pulled off the rock), MB—moderately buried, DB—deeply buried.

§ST—sample thickness.

#TSF—topographic shielding factor.

**^{10}Be/^{9}Be ratios were corrected for background ^{10}Be detected in full procedural blanks (Sar_F01−05, Men_F05: 1.87 ± 0.94 × 10^{-15}; Sis_F03, 04, Men_F07: 4.2 ± 0.17 × 10^{-15}; Tel_F05−09: 1.22 ± 0.43 × 10^{-15}; Men_F02−04,06: 17.0 ± 5.0 × 10^{-15}; KO20−23, Men_F01: 32.0 ± 2.0 × 10^{-15}). AMS—accelerator mass spectrometry.

††LSD age (internal/external errors quoted) was calculated using the Balco et al. (2008) calibration data set (^{10}Be decay constant of 5.1 ± 0.3 × 10^{-7}), and Lifton et al. (2014) calculation scheme with the Lifton 2016 VDM geomagnetic database. Production rate for the CREP calculator is 4.13 ± 0.2 ^{10}Be atoms/g SiO_2/yr (Martin et al., 2017) with a ^{10}Be half-life of 1.387 m.y., density of 2.7 g cm^3, AMS Standard of 07KNSTD. Ages were rounded to 1 decimal place.

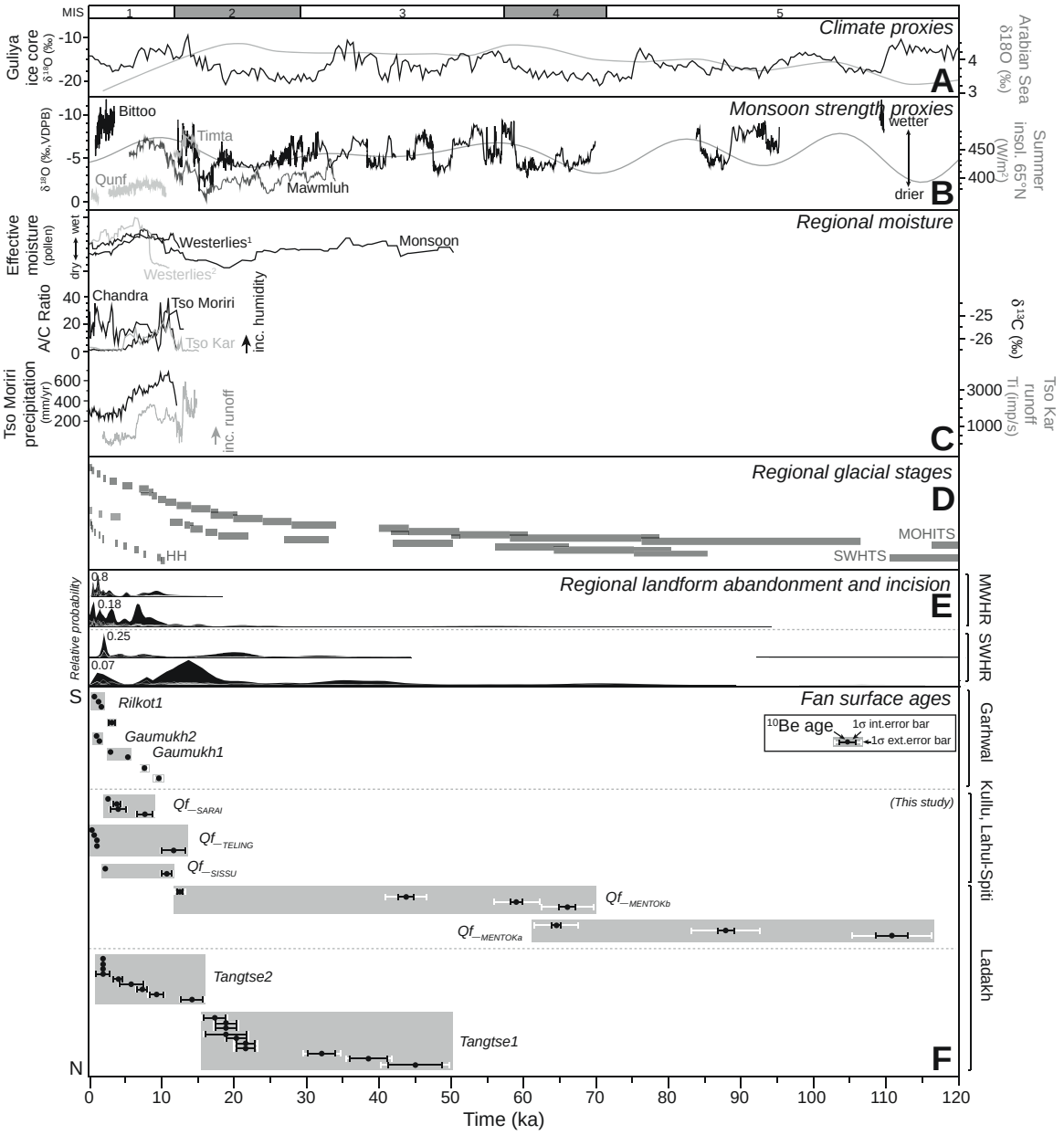

Figure 6. Late Quaternary paleoclimatic, paleoenvironmental, glacial, and geomorphic records for the NW Himalaya and Tibet. (A) Climatic proxies including the Guliya ice-core $\delta^{18}O$ record (Thompson et al., 1997) and the Arabian Sea core 722 $\delta^{18}O$ record (Clemens et al., 1996; Lisiecki and Raymo, 2005). MIS—marine oxygen isotope stage. (B) 65°N summer insolation (Leuschner and Sirocko, 2003; Berger and Loutre, 1991), and monsoon strength proxies including cave records from Qunf in Oman (Fleitmann et al., 2003), and Bittoo (Kathayat et al., 2016), Mawmluh (Dutt et al., 2015), and Timta (Sinha et al., 2005; VDPB—Vienna Peedee belemnite) in India. (C) A/C ratio—*Artemisia*-to-Chenopodiaceae pollen ratio. Regional moisture proxies including Central Asian pollen records of monsoon (Herzschuh, 2006) and midlatitude westerlies moisture transport ([1]Herzschuh, 2006, record; [2]Chen et al., 2008, record), and paleoenvironmental and paleohydrologic records for Tso Moriri (Leipe et al., 2014; Mishra et al., 2015), Tso Kar (Demske et al., 2009; Wünnemann et al., 2010), and $\delta^{13}C$ peat-lake sequence for the Chandra valley (Rawat et al., 2015). (D) Regional glacial stages for the NW Himalaya, with Himalayan Holocene (HH) stages from Saha et al. (2018), semiarid western Himalayan-Tibetan stages (SWHTS) from Dortch et al. (2013), and monsoonal Himalayan-Tibetan stages (MOHITS) from Murari et al. (2014). (E) Regional events of landform abandonment (upper) and incision (lower) for the NW Himalaya shown by probability density distribution plots for the monsoon-influenced western Himalaya ranges (MWHR; landform abandonment = Barnard et al., 2004a, 2004b; Scherler et al., 2015; incision = Barnard et al., 2004a, 2004b; Bookhagen et al., 2006; Adams et al., 2009; Dortch et al., 2011b; Dey et al., 2016) and semiarid western Himalaya ranges (SWHR; landform abandonment = Brown et al., 2002, 2003; Dortch et al., 2011b; Blöthe et al., 2014; incision = Leland et al., 1998; Brown et al., 2002, 2003; Seong et al., 2007; Dortch et al., 2011a, 2011b). Fan ^{10}Be ages from this study are not included in these probability density functions. (F) Fan chronologies for the NW Himalaya defined by terrestrial cosmogenic nuclide dating for Ladakh, Lahul-Spiti, and Kullu, and recalculated for Garhwal (Barnard et al., 2004a, 2004b) and northern Ladakh (Brown et al., 2002, 2003; Dortch et al., 2011c).

al., 2013) and the period of reduced monsoon strength and effective moisture associated with the LGM (Fig. 6).

The *Tangtse2* debris-flow fan formed after the Pangong Tso outburst flood at 11.1 ± 1.0 ka, which was a large flood event that reworked the majority of the landforms and sediment deposits that occupied the Tangtse valley floor at that time (Dortch et al., 2011c). The late-glacial ages for the fan surface therefore reflect inherited ^{10}Be. The remaining ^{10}Be ages suggest that *Tangtse2* was abandoned during the cooling temperatures and increasing aridity of the Mid- to Late Holocene (Fig. 6).

Fan Surface Abandonment throughout the NW Himalaya

The Mid- to Late Holocene fan surfaces of this study are predominantly limited to the debris-flow fans of the monsoon-influenced western Himalaya ranges region. The semiarid western Himalaya ranges region presents greater complexity, with the preservation of fan surfaces with abandonment ages from 110.8 ± 5.5 to 2.1 ± 0.3 ka. Preservation bias favors Holocene-aged fan surfaces in the monsoon-influenced western Himalaya ranges because elevated rates of erosion in this region rapidly rework and overprint landforms and sediment deposits over time scales of 10^4–10^1 yr (Gabet et al., 2004; Wulf et al., 2010; Murari et al., 2014). The lower rates of landscape change in the semiarid interior ranges help to preserve a longer fan record (Dortch et al., 2011a, 2011b; Dietsch et al., 2015; Jonell et al., 2018).

The source catchments of the debris-flow fans of this study have mean slopes >30°, above which slopes are unable to securely retain regolith, snow, or ice (Table 2). The steep topography of these catchments is conducive to diffusive hillslope processes, as well as stochastic high-magnitude mass-wasting events (Gruber and Haeberli, 2007; Dortch et al., 2009; Nagai et al., 2013). The narrow valley floor and steep-relief hillslopes of the Chandra valley restrict the extent to which the Qf_{-SISSU} and $Qf_{-TELING}$ fans can aggrade out into the trunk valley. The fans are further truncated and dissected by the Chandra River and tributaries. In contrast, the Karzok valley tributary catchments, which are of comparable size to the former, have shallower mean slopes (<20°) and channel profiles (10°), which allow for large, gently sloping (<8°) alluvial fans to aggrade throughout the valley (Table 2). These examples demonstrate the importance of topography in determining the type, size, and morphology of fans in the NW Himalaya.

With the exception of the Karzok fans, the timing of fan abandonment throughout the NW Himalaya coincided with periods of relative cooling and increasing aridity (Fig. 6). During warm, wet conditions, fans aggraded and evolved as sediment was released and then transferred throughout the catchments. As the climate then transitioned to cooler and drier conditions, aggradation ceased or became more restricted, and the fan surface stabilized. We note, however, that fans can also develop in response to single high-magnitude events such as storms and outburst floods or rapid fluctuations in precipitation (10^4–10^2 yr; Hasnain, 1996; Craddock et al., 2007; Wulf et al., 2010).

The fan surface ages coincide with one or more local glacial stages and between one and five regional glacial stages (Fig. 6). Periods of late Quaternary glaciation throughout the Himalayan-Tibetan orogen were cooler and drier than the present day (Burbank et al., 2003). Our study therefore proposes that fans evolved during interglacial periods or phases of deglaciation during a higher-intensity monsoon, and then as glacial conditions were reestablished, the fans stabilized. As an example, fan aggradation, which includes the monsoon-influenced western Himalaya range fans of this study, occurred in the NW Himalaya as part of the landscape response to a period of glacier retreat during the Mid-Holocene. This more restricted glaciation followed a time of extensive glacial advances during the Early Holocene, which has been argued to have resulted from the northerly migration of the Intertropical Convergence Zone and an enhanced summer monsoon (Fleitmann et al., 2003, 2007; Dykoski et al., 2005; Wang et al., 2005; Herzschuh, 2006; Hu et al., 2008; Leipe et al., 2014). Enhanced cooling due to the strengthening of the midlatitude westerlies by the Mid-Holocene likely caused a reduction in fan sedimentation and the stabilization and abandonment of fan surfaces. This example highlights the sensitivity of fans in the NW Himalaya to glacial advances and/or associated shifts in local-regional climate.

The nature and timing of fan evolution and abandonment in the NW Himalaya are determined by the interactions between climate and internal catchment dynamics such as topography, sediment supply, and catchment lithology. Seismic events or shifts in base level are additional external forcing mechanisms that may prompt further mass redistribution in these high-altitude settings (Owen et al., 1995; Hobley et al., 2010).

Regional Records of Landform Abandonment and Incision

The regional timing of landform abandonment for the semiarid western Himalaya ranges and monsoon-influenced western Himalaya ranges broadly accompanied periods of weakening monsoon and relative cooling (Fig. 6; Gasse et al., 1996; Fleitmann et al., 2003, 2007; Dykoski et al., 2005; Wang et al., 2005; Herzschuh, 2006; Hu et al., 2008; Dong et al., 2010; Leipe et al., 2014; Rawat et al., 2015; Hudson et al., 2016; Srivastava et al., 2017). This suggests that, on the regional scale, landforms aggrade and evolve during warm and wet conditions before a shift to cool arid conditions forces the stabilization and abandonment of the landforms. Regional incision events are less straightforward, as they are recognized across various climatic conditions. The ubiquitous nature of erosion in these active alpine settings is perhaps the reason for this complexity (Barnard et al., 2006b). The contrasting geomorphic regimes of the NW Himalaya cause a similar bias in the records of landform abandonment and incision in favor of Holocene events, as has been observed in the fan record of this study.

The $Qf_{-TELING}$, *Gaumukh2*, and *Tangtse1* fan surface ages overlap with regional events of landform abandonment for the monsoon-influenced western Himalaya ranges and semiarid

western Himalaya ranges regions, respectively (Fig. 6). A greater correspondence is evident, however, between the fans of this study and regional incision events. This correlation is likely because of the greater number of incision records available in the NW Himalaya compared to landform abandonment records. Some landform abandonment and incision events within the regions of the monsoon-influenced western Himalaya ranges (landform abandonment at 1.4 ± 0.5 ka, incision at 1.0 ± 0.1 ka) and the semiarid western Himalaya ranges (landform abandonment at 31.5 ± 5.1 ka, incision at 35.9 ± 5.9 ka) were synchronous. This alludes to the existence of region-scale cycles of aggradation and incision throughout the NW Himalaya. Unlike parts of the Himalaya and other mountain systems, cycles of aggradation and incision at particular intervals (i.e., 40 or 100 k.y. cycles) have not been recognized in the NW Himalaya (Pratt et al., 2002; Srivastava et al., 2008; Kumar and Srivastava, 2017; Tofelde et al., 2017).

The landform abandonment and incision events in the monsoon-influenced and semiarid western Himalaya ranges each occurred alongside two to seven regional glacial stages (monsoon-influenced western Himalaya ranges landform abandonment [MOHITS 1B, 1C; Himalayan Holocene HH1, 2] and incision [MOHITS 1C–1K; HH1, 2, 4–7]; semiarid western Himalaya–Tibetan orogen landform abandonment [SWHTS 2D–2F] and incision [SWHTS 1B, 1C, 2A–2D, 2F; HH2, 3]; Dortch et al., 2013; Murari et al., 2014; Saha et al., 2018; Fig. 6). This overlap is anticipated due to the duration of these geomorphic events, and the number of glacial records available throughout the inherently glaciated NW Himalaya. The most significant regional incision event for both monsoon-influenced and semiarid western Himalaya ranges occurred at the time of extensive glaciation at the onset and early millennia of the Holocene (Fig. 6). This incision event likely reflects enhanced glacial and fluvial erosion during this glaciation and its association phase of deglaciation. More broadly, these regional records of geomorphic change illustrate the climatic dependence of landscape change throughout the NW Himalaya.

CONCLUSION

This study defined the timing of fan surface abandonment for 10 fans in the NW Himalaya; fan surface ages range from 110.8 ± 5.5–64.5 ± 2.9 ka to 1.8 ± 0.2–0.9 ± 0.1 ka. Debris-flow fans in the Garhwal, Kullu, and Lahul-Spiti regions of the monsoon-influenced Greater Himalaya were largely abandoned during the Holocene. In the Ladakh region of the Greater and Tethyan Himalaya, large alluvial fans and debris-flow fans have surface ages that extend throughout the last glacial. The type, size, and morphology of the fans were influenced by the topography and fluvial channel behaviors of the source catchments and trunk valleys.

We defined the regional landform abandonment and incision events for the monsoon-influenced and semiarid western Himalaya ranges for the past ~120 k.y. In the monsoon-influenced western Himalaya ranges, regional geomorphic events were restricted to the Holocene, while in the semiarid western Himalaya ranges, they were recognized from ca. 40 ka. The fans of this study and the regional geomorphic records showed preservation bias, where elevated rates of erosion and sediment reworking in the monsoon-influenced western Himalaya ranges mean that the landforms retained in these catchments are restricted to the Holocene. The lower rates of landscape change in the semiarid western Himalaya ranges enable the preservation of longer geomorphic records.

The timing of fan surface abandonment for the 10 fans of this study and the regional events of landform abandonment throughout the NW Himalaya accompanied periods of weakening monsoon strength and relative cooling. The landforms aggraded and evolved during warm-wet conditions before a shift to cool and arid conditions forced the stabilization and abandonment of the landforms. Regional incision events were recognized across various climatic conditions throughout the late Quaternary, likely due to the ubiquitous nature of erosion in these active alpine settings.

The fan surface ages were coincident with one or more local glacial stages and between one and five regional glacial stages. Fan formation and evolution extended throughout interglacial periods and times of deglaciation before stabilizing once cool-arid glacial conditions returned. The nature and timing of the fan evolution and abandonment were determined by the interaction between internal catchment dynamics and climate. Regional geomorphic events defined for the monsoon-influenced western Himalaya ranges and semiarid western Himalaya ranges also coincided with between two and seven regional glacial stages. This further illustrates the critical role played by glaciation and glacial processes in local and regional landscape change. More broadly, this study demonstrates the importance of climate-driven processes in the sediment flux and topographic evolution of the NW Himalaya.

ACKNOWLEDGMENTS

Orr and Owen thank the University of Cincinnati for providing tuition and stipend to support this work as part of Orr's doctoral thesis and for the processing of samples for ^{10}Be dating. Orr and Saha thank the Geological Society of America and the Graduate Student Governance Association, University of Cincinnati, for research grants to conduct fieldwork. Caffee acknowledges support from the National Science Foundation (EAR-1560658). We also thank Paul Bierman, Nick Lancaster, and Alan Gillespie for their detailed, constructive suggestions and comments on our manuscript.

REFERENCES CITED

Adams, B., Dietsch, C., Owen, L.A., Caffee, M.W., Spotila, J., and Haneberg, W.C., 2009, Exhumation and incision history of the Lahul Himalaya, northern India, based on (U-Th)/He thermochronometry and terrestrial cosmogenic nuclide methods: Geomorphology, v. 107, no. 3–4, p. 285–299, https://doi.org/10.1016/j.geomorph.2008.12.017.

Azam, M.F., Wagnon, P., Vincent, C., Ramanathan, A.L., Favier, V., Mandal, A., and Pottakkal, J.G., 2014, Processes governing the mass balance

of Chhota Shigri Glacier (western Himalaya, India) assessed by point-scale surface energy balance measurements: The Cryosphere, v. 8, no. 6, p. 2195–2217, https://doi.org/10.5194/tc-8-2195-2014.

Balco, G., Stone, J., Lifton, N., and Dunai, T., 2008, A complete and easily accessible means of calculating surface exposure ages or erosion rates from ^{10}Be and ^{26}Al measurements: Quaternary Geochronology, v. 3, p. 174–195, https://doi.org/10.1016/j.quageo.2007.12.001.

Ballantyne, C.K., 2002a, Paraglacial geomorphology: Quaternary Science Reviews, v. 21, no. 18–19, p. 1935–2017, https://doi.org/10.1016/S0277-3791(02)00005-7.

Ballantyne, C.K., 2002b, A general model of paraglacial landscape response: The Holocene, v. 12, no. 3, p. 371–376, https://doi.org/10.1191/0959683602hl553fa.

Barnard, P.L., Owen, L.A., Sharma, M.C., and Finkel, R.C., 2001, Natural and human-induced landsliding in the Garhwal Himalaya of northern India: Geomorphology, v. 40, no. 1–2, p. 21–35, https://doi.org/10.1016/S0169-555X(01)00035-6.

Barnard, P., Owen, L., and Finkel, R., 2004a, Style and timing of glacial and paraglacial sedimentation in a monsoon-influenced High Himalayan environment, the upper Bhagirathi Valley, Garhwal Himalaya: Sedimentary Geology, v. 165, p. 199–221, https://doi.org/10.1016/j.sedgeo.2003.11.009.

Barnard, P.L., Owen, L.A., Sharma, M.C., and Finkel, R.C., 2004b, Late Quaternary (Holocene) landscape evolution of a monsoon-influenced High Himalayan valley, Gori Ganga, Nanda Devi, NE Garhwal: Geomorphology, v. 61, no. 1–2, p. 91–110, https://doi.org/10.1016/j.geomorph.2003.12.002.

Barnard, P.L., Owen, L., Finkel, R., and Asahi, K., 2006a, Landscape response to deglaciation in a high relief, monsoon-influenced alpine environment, Langtang Himal, Nepal: Quaternary Science Reviews, v. 25, p. 2162–2176, https://doi.org/10.1016/j.quascirev.2006.02.002.

Barnard, P.L., Owen, L.A., and Finkel, R.C., 2006b, Quaternary fans and terraces in the Khumbu Himal south of Mount Everest: Their characteristics, age and formation: Journal of the Geological Society, v. 163, no. 2, p. 383–399, https://doi.org/10.1144/0016-764904-157.

Benn, D., and Owen, L., 1998, The role of the Indian summer monsoon and the mid-latitude westerlies in Himalayan glaciation: A review and speculative discussion: Journal of the Geological Society, v. 155, p. 353–363, https://doi.org/10.1144/gsjgs.155.2.0353.

Benn, D.I., and Owen, L.A., 2002, Himalayan glacial sedimentary environments: A framework for reconstructing and dating former glacial extents in high mountain regions: Quaternary International, v. 97–98, p. 3–25, https://doi.org/10.1016/S1040-6182(02)00048-4.

Berger, A., and Loutre, M.F., 1991, Insolation values for the climate of the last 10 million years: Quaternary Science Reviews, v. 10, no. 4, p. 297–317, https://doi.org/10.1016/0277-3791(91)90033-Q.

Blisniuk, K., Oskin, M., Fletcher, K., Rockwell, T., and Sharp, W., 2012, Assessing the reliability of U-series and ^{10}Be dating techniques on alluvial fans in the Anza Borrego Desert, California: Quaternary Geochronology, v. 13, p. 26–41, https://doi.org/10.1016/j.quageo.2012.08.004.

Blöthe, J.H., Munack, H., Korup, O., Fülling, A., Garzanti, E., Resentini, A., and Kubik, P.W., 2014, Late Quaternary valley infill and dissection in the Indus River, western Tibetan Plateau margin: Quaternary Science Reviews, v. 94, p. 102–119, https://doi.org/10.1016/j.quascirev.2014.04.011.

Bookhagen, B., and Burbank, D., 2006, Topography, relief and TRMM-derived rainfall variations along the Himalaya: Geophysical Research Letters, v. 33, L08405, https://doi.org/10.1029/2006GL026037.

Bookhagen, B., and Burbank, D., 2010, Toward a complete Himalayan hydrological budget: Spatiotemporal distribution of snowmelt and rainfall and their impact on river discharge: Journal of Geophysical Research, v. 115, no. F3, F03019, https://doi.org/10.1029/2009JF001426.

Bookhagen, B., Thiede, R., and Strecker, M., 2005, Late Quaternary intensified monsoon phases control landscape evolution in the northwest Himalaya: Geology, v. 33, no. 2, p. 149–152, https://doi.org/10.1130/G20982.1.

Bookhagen, B., Fleitmann, D., Nishiizumi, K., Strecker, M.R., and Thiede, R.C., 2006, Holocene monsoonal dynamics and fluvial terrace formation in the northwest Himalaya, India: Geology, v. 34, no. 7, p. 601–604, https://doi.org/10.1130/G22698.1.

Brown, E.T., Bendick, R., Bourles, D.L., Gaur, V., Molnar, P., Raisbeck, G.M., and Yiou, F., 2002, Slip rates of the Karakorum fault, Ladakh, India, determined using cosmic ray exposure dating of debris flows and moraines: Journal of Geophysical Research–Solid Earth, v. 107, no. B9, 2192, https://doi.org/10.1029/2000JB000100.

Brown, E.T., Bendick, R., Bourles, D.L., Gaur, V., Molnar, P., Raisbeck, G.M., and Yiou, F., 2003, Early Holocene climate recorded in geomorphological features in western Tibet: Palaeogeography, Palaeoclimatology, Palaeoecology, v. 199, no. 1–2, p. 141–151, https://doi.org/10.1016/S0031-0182(03)00501-7.

Burbank, D.W., Leland, J., Fielding, E., Anderson, R.S., Brozovic, N., Reid, M.R., and Duncan, C., 1996, Bedrock incision, rock uplift and threshold hillslopes in the northwestern Himalayas: Nature, v. 379, no. 6565, p. 505–510, https://doi.org/10.1038/379505a0.

Burbank, D., Blythe, A., Putkonen, J., Pratt-Sitaula, B., Gabet, E., Oskin, M., Barros, A., and Ojha, T., 2003, Decoupling of erosion and precipitation in the Himalayas: Nature, v. 426, p. 652–655, https://doi.org/10.1038/nature02187.

Cesta, J.M., and Ward, D.J., 2016, Timing and nature of alluvial fan development along the Chajnantor Plateau, northern Chile: Geomorphology, v. 273, p. 412–427, https://doi.org/10.1016/j.geomorph.2016.09.003.

Chen, F., Yu, Z., Yang, M., Ito, E., Wang, S., Madsen, D.B., Huang, X., Zhao, Y., Sato, T., Birks, H.J.B., and Boomer, I., 2008, Holocene moisture evolution in arid Central Asia and its out-of-phase relationship with Asian monsoon history: Quaternary Science Reviews, v. 27, no. 3–4, p. 351–364, https://doi.org/10.1016/j.quascirev.2007.10.017.

Clemens, S.C., Murray, D.W., and Prell, W.L., 1996, Nonstationary phase of the Plio-Pleistocene Asian monsoon: Science, v. 274, no. 5289, p. 943–948, https://doi.org/10.1126/science.274.5289.943.

Clift, P.D., Carter, A., Giosan, L., Durcan, J., Duller, G.A.T., Macklin, M.G., Alizai, A., Tabrez, A.R., Danish, M., VanLaningham, S., and Fuller, D.Q., 2012, U-Pb zircon dating evidence for a Pleistocene Sarasvati River and capture of the Yamuna River: Geology, v. 40, p. 211–214, https://doi.org/10.1130/G32840.1.

Craddock, W.H., Burbank, D.W., Bookhagen, B., and Gabet, E.J., 2007, Bedrock channel geometry along an orographic rainfall gradient in the upper Marsyandi River valley in central Nepal: Journal of Geophysical Research–Earth Surface, v. 112, no. F3, F03007, https://doi.org/10.1029/2006JF000589.

Demske, D., Tarasov, P.E., Wünnemann, B., and Riedel, F., 2009, Late glacial and Holocene vegetation, Indian monsoon and westerly circulation in the Trans-Himalaya recorded in the lacustrine pollen sequence from Tso Kar, Ladakh, NW India: Palaeogeography, Palaeoclimatology, Palaeoecology, v. 279, no. 3–4, p. 172–185, https://doi.org/10.1016/j.palaeo.2009.05.008.

Derbyshire, E., and Owen, L.A., 1990, Quaternary alluvial fans in the Karakoram Mountains, *in* Rachocki, A.H., and Church, M., eds., Alluvial Fans: A Field Approach: Chichester, UK, Wiley, p. 27–53.

Dey, S., Thiede, R.C., Schildgen, T.F., Wittmann, H., Bookhagen, B., Scherler, D., Jain, V., and Strecker, M.R., 2016, Climate-driven sediment aggradation and incision since the late Pleistocene in the NW Himalaya, India: Earth and Planetary Science Letters, v. 449, p. 321–331, https://doi.org/10.1016/j.epsl.2016.05.050.

Dietsch, C., Dortch, J., Reynhout, S., Owen, L., and Caffee, M., 2015, Very slow erosion and topographic evolution of the southern Ladakh Range, India: Earth Surface Processes and Landforms, v. 40, no. 3, p. 389–402, https://doi.org/10.1002/esp.3640.

Dong, J., Wang, Y., Cheng, H., Hardt, B., Edwards, R.L., Kong, X., Wu, J., Chen, S., Liu, D., Jiang, X., and Zhao, K., 2010, A high-resolution stalagmite record of the Holocene East Asian monsoon from Mt. Shennongjia, central China: The Holocene, v. 20, p. 257–264, https://doi.org/10.1177/0959683609350393.

Dortch, J.M., Owen, L.A., Haneberg, W.C., Caffee, M.W., Dietsch, C., and Kamp, U., 2009, Nature and timing of large landslides in northern India: Quaternary Science Reviews, v. 28, p. 1037–1054, https://doi.org/10.1016/j.quascirev.2008.05.002.

Dortch, J.M., Dietsch, C., Owen, L.A., Caffee, M.W., and Ruppert, K., 2011a, Episodic fluvial incision of rivers and rock uplift in the Himalaya and Transhimalaya: Journal of the Geological Society, v. 168, no. 3, p. 783–804, https://doi.org/10.1144/0016-76492009-158.

Dortch, J., Owen, L., Schoenbohm, L., and Caffee, M., 2011b, Asymmetrical erosion and morphological development of the central Ladakh Range, northern India: Geomorphology, v. 135, p. 167–180, https://doi.org/10.1016/j.geomorph.2011.08.014.

Dortch, J.M., Owen, L.A., Caffee, M.W., and Kamp, U., 2011c, Catastrophic partial drainage of Pangong Tso, northern India and Tibet: Geomorphology, v. 125, no. 1, p. 109–121, https://doi.org/10.1016/j.geomorph.2010.08.017.

Dortch, J., Owen, L., and Caffee, M., 2013, Timing and climatic drivers for glaciation across semi-arid western Himalayan-Tibetan orogen: Quaternary Science Reviews, v. 78, p. 188–208, https://doi.org/10.1016/j.quascirev.2013.07.025.

Dühnforth, M., Densmore, A.L., Ivy-Ochs, S., Allen, P.A., and Kubik, P.W., 2007, Timing and patterns of debris flow deposition on Shepherd and Symmes Creek fans, Owens Valley, California, deduced from cosmogenic ^{10}Be: Journal of Geophysical Research–Earth Surface, v. 112, no. F3, F03S15, https://doi.org/10.1029/2006JF000562.

Dutt, S., Gupta, A.K., Clemens, S.C., Cheng, H., Singh, R.K., Kathayat, G., and Edwards, R.L., 2015, Abrupt changes in Indian summer monsoon strength during 33,800 to 5500 years BP: Geophysical Research Letters, v. 42, p. 5526–5532, https://doi.org/10.1002/2015GL064015.

Dykoski, C.A., Edwards, R.L., Cheng, H., Yuan, D., Cai, Y., Zhang, M., Lin, Y., Qing, J., An, Z., and Revenaugh, J., 2005, A high-resolution, absolute-dated Holocene and deglacial Asian monsoon record from Dongge Cave, China: Earth and Planetary Science Letters, v. 233, p. 71–86, https://doi.org/10.1016/j.epsl.2005.01.036.

Eppes, M.C., and McFadden, L., 2008, The influence of bedrock weathering on the response of drainage basins and associated alluvial fans to Holocene climates, San Bernardino Mountains, California, USA: The Holocene, v. 18, no. 6, p. 895–905, https://doi.org/10.1177/0959683608093526.

Eugster, P., Scherler, D., Thiede, R.C., Codilean, A.T., and Strecker, M.R., 2016, Rapid Last Glacial Maximum deglaciation in the Indian Himalaya coeval with midlatitude glaciers: New insights from ^{10}Be-dating of ice-polished bedrock surfaces in the Chandra Valley, NW Himalaya: Geophysical Research Letters, v. 43, no. 4, p. 1589–1597, https://doi.org/10.1002/2015GL066077.

Fleitmann, D., Burns, S.J., Mudelsee, M., Neff, U., Kramers, J., Mangini, A., and Matter, A., 2003, Holocene forcing of the Indian monsoon recorded in a stalagmite from southern Oman: Science, v. 300, p. 1737–1739, https://doi.org/10.1126/science.1083130.

Fleitmann, D., Burns, S.J., Mangini, A., Mudelsee, M., Kramers, J., Villa, I., Neff, U., Al-Subbary, A.A., Buettner, A., Hippler, D., and Matter, A., 2007, Holocene ITCZ and Indian monsoon dynamics recorded in stalagmites from Oman and Yemen (Socotra): Quaternary Science Reviews, v. 26, p. 170–188, https://doi.org/10.1016/j.quascirev.2006.04.012.

Gabet, E.J., Burbank, D.W., Putkonen, J.K., Pratt-Sitaula, B.A., and Ojha, T., 2004, Rainfall thresholds for landsliding in the Himalayas of Nepal: Geomorphology, v. 63, no. 3–4, p. 131–143, https://doi.org/10.1016/j.geomorph.2004.03.011.

Gasse, F., Fontes, J.C., Van Campo, E., and Wei, K., 1996, Holocene environmental changes in Bangong Co basin (Western Tibet). Part 4: Discussion and conclusions: Palaeogeography, Palaeoclimatology, Palaeoecology, v. 120, no. 1–2, p. 79–92, https://doi.org/10.1016/0031-0182(95)00035-6.

GeoMappApp, 2014, Marine Geoscience Data System: GeoMappApp, http://www.geomappap.org (accessed 21 August 2014).

Gosse, J., McDonald, E., and Finkel, R., 2003, Cosmogenic nuclide dating of arid region alluvial fans: Geological Society of America Abstracts with Programs, v. 35, no. 3, p. 8.

Gruber, S., and Haeberli, W., 2007, Permafrost in steep bedrock slopes and its temperature-related destabilization following climate change: Journal of Geophysical Research–Earth Surface, v. 112, no. F2, F02S18, https://doi.org/10.1029/2006JF000547.

Gusain, H.S., Singh, A., Ganju, A., and Singh, D., 2004. Characteristics of the seasonal snow-cover of Pir Panjal and Great Himalayan ranges in Indian Himalaya, *in* Proceedings of the International Symposium on Snow Monitoring and Avalanches 2004: Manali, India, p. 97–102.

Hales, T.C., and Roering, J.J., 2007, Climatic controls on frost cracking and implications for the evolution of bedrock landscapes: Journal of Geophysical Research–Earth Surface, v. 112, no. F2, F02033, https://doi.org/10.1029/2006JF000616.

Hasnain, S.I., 1996, Factors controlling suspended sediment transport in Himalayan glacier meltwaters: Journal of Hydrology, v. 181, no. 1–4, p. 49–62, https://doi.org/10.1016/0022-1694(95)02917-6.

Hedrick, K., Seong, Y., Owen, L., Caffee, M., and Dietsch, C., 2011, Towards defining the transition in style and timing of Quaternary glaciation between the monsoon-influenced Greater Himalaya and the semi-arid Transhimalaya of northern India: Quaternary International, v. 236, p. 21–33, https://doi.org/10.1016/j.quaint.2010.07.023.

Hedrick, K., Owen, L.A., Rockwell, T.K., Meigs, A., Costa, C., Caffee, M.W., Masana, E., and Ahumada, E., 2013, Timing and nature of alluvial fan and strath terrace formation in the Eastern Precordillera of Argentina: Quaternary Science Reviews, v. 80, p. 143–168, https://doi.org/10.1016/j.quascirev.2013.05.004.

Heimsath, A.M., and McGlynn, R., 2008, Quantifying periglacial erosion in the Nepal High Himalaya: Geomorphology, v. 97, no. 1–2, p. 5–23, https://doi.org/10.1016/j.geomorph.2007.02.046.

Herzschuh, U., 2006, Palaeo-moisture evolution in monsoonal Central Asia during the last 50,000 years: Quaternary Science Reviews, v. 25, no. 1–2, p. 163–178, https://doi.org/10.1016/j.quascirev.2005.02.006.

Hewitt, K., 2009, Glacially conditioned rock-slope failures and disturbance-regime landscapes, Upper Indus Basin, northern Pakistan, *in* Knight, J., and Harrison, S., eds., Periglacial and Paraglacial Processes and Environments: Geological Society, London, Special Publication 320, p. 235–255, https://doi.org/10.1144/SP320.15.

Heyman, J., Stroeven, A., Harbor, J., and Caffee, M., 2011, Too young or too old: Evaluating cosmogenic exposure dating based on an analysis of compiled boulder exposure ages: Earth and Planetary Science Letters, v. 302, p. 71–80, https://doi.org/10.1016/j.epsl.2010.11.040.

Hobley, D., Sinclair, H., and Cowie, P., 2010, Processes, rates, and timescales of fluvial response in an ancient postglacial landscape of the northwest Indian Himalaya: Geological Society of America Bulletin, v. 122, p. 1569–1584, https://doi.org/10.1130/B30048.1.

Hu, C., Henderson, G.M., Huang, J., Xie, S., Sun, Y., and Johnson, K.R., 2008, Quantification of Holocene Asian monsoon rainfall from spatially separated cave records: Earth and Planetary Science Letters, v. 266, p. 221–232, https://doi.org/10.1016/j.epsl.2007.10.015.

Hudson, A.M., Olsen, J.W., Quade, J., Lei, G., Huth, T.E., and Zhang, H., 2016, A regional record of expanded Holocene wetlands and prehistoric human occupation from paleowetland deposits of the western Yarlung Tsangpo valley, southern Tibetan Plateau: Quaternary Research, v. 86, p. 13–33, https://doi.org/10.1017/j.yqres.2016.04.001.

Hughes, P., 2010, Geomorphology and Quaternary stratigraphy: The roles of morpho-, litho- and allostratigraphy: Geomorphology, v. 123, p. 189–199, https://doi.org/10.1016/j.geomorph.2010.07.025.

Hughes, P., Gibbard, P., and Woodwad, J., 2005, Quaternary glacial records in mountain regions: A formal stratigraphical approach: Episodes, v. 28, p. 85–92, https://doi.org/10.18814/epiiugs/2005/v28i2/002.

Jonell, T.N., Owen, L.A., Carter, A., Schwenniger, J.L., and Clift, P.D., 2018, Quantifying episodic erosion and transient storage on the western margin of the Tibetan Plateau, upper Indus River: Quaternary Research, v. 89, p. 281–306, https://doi.org/10.1017/qua.2017.92.

Jones, P.D., Lister, D.H., Osborn, T.J., Harpham, C., Salmon, M., and Morice, C.P., 2012, Hemispheric and large-scale land-surface air temperature variations: An extensive revision and an update to 2010: Journal of Geophysical Research, ser. D, Atmospheres, v. 117, no. D5, D05127, https://doi.org/10.1029/2011JD017139.

Kathayat, G., Cheng, H., Sinha, A., Spötl, C., Edwards, R.L., Zhang, H., Li, X., Yi, L., Ning, Y., Cai, Y., and Lui, W.L., 2016, Indian monsoon variability on millennial-orbital timescales: Scientific Reports, v. 6, 24374, https://doi.org/10.1038/srep24374.

Kohl, C.P., and Nishiizumi, K., 1992, Chemical isolation of quartz for measurement of in situ produced cosmogenic nuclides: Geochimica et Cosmochimica Acta, v. 56, p. 3583–3587, https://doi.org/10.1016/0016-7037(92)90401-4.

Kumar, A., and Srivastava, P., 2017, The role of climate and tectonics in aggradation and incision of the Indus River in the Ladakh Himalaya during the late Quaternary: Quaternary Research, v. 87, no. 3, p. 363–385, https://doi.org/10.1017/qua.2017.19.

Kumar Singh, A., Parkash, B., Mohindra, R., Thomas, J.V., and Singhvi, A.K., 2001, Quaternary alluvial fan sedimentation in the Dehradun valley piggyback basin, NW Himalaya: Tectonic and palaeoclimatic implications: Basin Research, v. 13, no. 4, p. 449–471, https://doi.org/10.1046/j.0950-091x.2001.00160.x.

Lavé, J., and Avouac, J.P., 2001, Fluvial incision and tectonic uplift across the Himalayas of central Nepal: Journal of Geophysical Research–Solid Earth, v. 106, no. B11, p. 26,561–26,591, https://doi.org/10.1029/2001JB000359.

Leipe, C., Demske, D., and Tarasov, P.E., 2014, A Holocene pollen record from the northwestern Himalayan lake Tso Moriri: Implications for palaeoclimatic and archaeological research: Quaternary International, v. 348, p. 93–112, https://doi.org/10.1016/j.quaint.2013.05.005.

Leland, J., Reid, M.R., Burbank, D.W., Finkel, R., and Caffee, M., 1998, Incision and differential bedrock uplift along the Indus River near Nanga

Parbat, Pakistan Himalaya, from ^{10}Be and ^{26}Al exposure age dating of bedrock straths: Earth and Planetary Science Letters, v. 154, no. 1–4, p. 93–107, https://doi.org/10.1016/S0012-821X(97)00171-4.

Leuschner, D., and Sirocko, F., 2003, Orbital insolation forcing of the Indian Monsoon—A motor for global climate changes?: Palaeogeography, Palaeoclimatology, Palaeoecology, v. 197, p. 83–95, https://doi.org/10.1016/S0031-0182(03)00387-0.

Lifton, N., Sato, T., and Dunai, T., 2014, Scaling in situ cosmogenic nuclide production rates using analytical approximations to atmospheric cosmic-ray fluxes: Earth and Planetary Science Letters, v. 386, p. 149–160, https://doi.org/10.1016/j.epsl.2013.10.052.

Lisiecki, L., and Raymo, M., 2005, A Pliocene–Pleistocene stack of 57 globally distributed benthic δ^{18}O records: Paleoceanography, v. 20, PA1003, https://doi.org/10.1029/2004PA001071.

Liu, X., and Dong, B., 2013, Influence of the Tibetan Plateau uplift on the Asian monsoon–arid environment evolution: Chinese Science Bulletin, v. 58, no. 34, p. 4277–4291, https://doi.org/10.1007/s11434-013-5987-8.

Martin, L., Blard, P., Balco, G., and Laurent, V., 2017, The CREp program and the ICE-D production rate calibration database: A fully parameterizable and updated online tool to compute cosmic-ray exposure ages: Quaternary Geochronology, v. 38, p. 25–49, https://doi.org/10.1016/j.quageo.2016.11.006.

Mishra, P.K., Anoop, A., Schettler, G., Prasad, S., Jehangir, A., Menzel, P., Naumann, R., Yousuf, A.R., Basavaiah, N., Deenadayalan, K., and Wiesner, M.G., 2015, Reconstructed late Quaternary hydrological changes from Lake Tso Moriri, NW Himalaya: Quaternary International, v. 371, p. 76–86, https://doi.org/10.1016/j.quaint.2014.11.040.

Mix, A.C., Bard, E., and Schneider, R., 2001, Environmental processes of the ice age: Land, ocean, glaciers (EPILOG): Quaternary Science Reviews, v. 20, p. 627–657, https://doi.org/10.1016/S0277-3791(00)00145-1.

Mölg, T., Maussion, F., and Scherer, D., 2014, Mid-latitude westerlies as a driver of glacier variability in monsoonal High Asia: Nature Climate Change, v. 4, no. 1, p. 68, https://doi.org/10.1038/nclimate2055.

Murari, M.K., Owen, L.A., Dortch, J.M., Caffee, M.W., Dietsch, C., Fuchs, M., Haneberg, W.C., Sharma, M.C., and Townsend-Small, A., 2014, Timing and climatic drivers for glaciation across monsoon-influenced regions of the Himalayan–Tibetan orogen: Quaternary Science Reviews, v. 88, p. 159–182, https://doi.org/10.1016/j.quascirev.2014.01.013.

Nagai, H., Fujita, K., Nuimura, T., and Sakai, A., 2013, Southwest-facing slopes control the formation of debris-covered glaciers in the Bhutan Himalaya: The Cryosphere, v. 7, no. 4, p. 1303–1314, https://doi.org/10.5194/tc-7-1303-2013.

Nicholas, A.P., and Quine, T.A., 2007, Modeling alluvial landform change in the absence of external environmental forcing: Geology, v. 35, no. 6, p. 527–530, https://doi.org/10.1130/G23377A.1.

Nishiizumi, K., Finkel, R.C., Caffee, M.W., Southon, J.R., Kohl, C.P., Arnold, J.R., Olinger, C.T., Poths, J., and Klein, J., 1994. Cosmogenic production of ^{10}Be and ^{26}Al on the surface of the Earth and underground, *in* Lanphere, M.A., Dalrymple, G.B., and Turrin, B.D., eds., Eighth International Conference on Geochronology, Cosmochronology and Isotope Geology: U.S. Geological Survey Circular 1107, p. 234, https://doi.org/10.1016/j.nimb.2007.01.297.

Orr, E., Owen, L., Murari, M., Saha, S., and Caffee, M., 2017, The timing and extent of Quaternary glaciation of Stok, northern Zanskar Range, Transhimalaya, of northern India: Geomorphology, v. 284, p. 142–155, https://doi.org/10.1016/j.geomorph.2016.05.031.

Orr, E.N., Owen, L.A., Saha, S., Caffee, M.W., and Murari, M.K., 2018, Quaternary glaciation of the Lato Massif, Zanskar Range of the NW Himalaya: Quaternary Science Reviews, v. 183, p. 140–156, https://doi.org/10.1016/j.quascirev.2018.01.005.

Orr, E.N., Owen, L.A., Saha, S., and Caffee, M.W., 2019, Rates of rockwall slope erosion in the upper Bhagirathi catchment, Garhwal Himalaya: Earth Surface Processes and Landforms, v. 44, no. 15, p. 3108–3127, https://doi.org/10.1002/esp.4720.

Osborn, T.J., and Jones, P., 2014, The CRUTEM4 land-surface air temperature data set: Construction, previous versions and dissemination via Google Earth: Earth System Science Data, v. 6, no. 1, p. 61–68, https://doi.org/10.5194/essd-6-61-2014.

Owen, L.A., 2009, Latest Pleistocene and Holocene glacier fluctuations in the Himalaya and Tibet: Quaternary Science Reviews, v. 28, no. 21–22, p. 2150–2164, https://doi.org/10.1016/j.quascirev.2008.10.020.

Owen, L.A., and Dortch, J.M., 2014, Nature and timing of Quaternary glaciation in the Himalayan-Tibetan orogen: Quaternary Science Reviews, v. 88, p. 14–54, https://doi.org/10.1016/j.quascirev.2013.11.016.

Owen, L.A., and Sharma, M.C., 1998, Rates and magnitudes of paraglacial fan formation in the Garhwal Himalaya: Implications for landscape evolution: Geomorphology, v. 26, no. 1–3, p. 171–184, https://doi.org/10.1016/S0169-555X(98)00057-9.

Owen, L.A., Benn, D.I., Derbyshire, E., Evans, D.J.A., Mitchell, W.A., Thompson, D., Richardson, S., Lloyd, M., and Holden, C., 1995, The geomorphology and landscape evolution of the Lahul Himalaya, northern India: Zeitschrift für Geomorphologie, v. 39, p. 145–174, https://ci.nii.ac.jp/naid/10009483085/.

Owen, L.A., Gualtieri, L.Y.N., Finkel, R.C., Caffee, M.W., Benn, D.I., and Sharma, M.C., 2001, Cosmogenic radionuclide dating of glacial landforms in the Lahul Himalaya, northern India: Defining the timing of late Quaternary glaciation: Journal of Quaternary Science, v. 16, no. 6, p. 555–563, https://doi.org/10.1002/jqs.621.

Owen, L.A., Frankel, K.L., Knott, J.R., Reynhout, S., Finkel, R.C., Dolan, J.F., and Lee, J., 2011, Beryllium-10 terrestrial cosmogenic nuclide surface exposure dating of Quaternary landforms in Death Valley: Geomorphology, v. 125, no. 4, p. 541–557, https://doi.org/10.1016/j.geomorph.2010.10.024.

Owen, L.A., Clemmens, S.J., Finkel, R.C., and Gray, H., 2014, Late Quaternary alluvial fans at the eastern end of the San Bernardino Mountains, Southern California: Quaternary Science Reviews, v. 87, p. 114–134, https://doi.org/10.1016/j.quascirev.2014.01.003.

Pope, R.J., and Wilkinson, K.N., 2005, Reconciling the roles of climate and tectonics in late Quaternary fan development on the Spartan piedmont, Greece, *in* Harvey, A.M., Mather, A.E., and Stokes, M., eds., Alluvial Fans: Geological Society, London, Special Publication 251, p. 133–152, https://doi.org/10.1144/GSL.SP.2005.251.01.10.

Pratt, B., Burbank, D.W., Heimsath, A., and Ojha, T., 2002, Impulsive alluviation during early Holocene strengthened monsoons, central Nepal Himalaya: Geology, v. 30, no. 10, p. 911–914, https://doi.org/10.1130/0091-7613(2002)030<0911:IADEHS>2.0.CO;2.

Prell, W.L., and Kutzbach, J.E., 1987, Monsoon variability over the past 150,000 years: Journal of Geophysical Research: Atmospheres, v. 92, no. D7, p. 8411–8425, https://doi.org/10.1029/JD092iD07p08411.

Qiang, X.K., Li, Z.X., Powell, C.M., and Zheng, H.B., 2001, Magnetostratigraphic record of the late Miocene onset of the East Asian monsoon, and Pliocene uplift of northern Tibet: Earth and Planetary Science Letters, v. 187, no. 1–2, p. 83–93, https://doi.org/10.1016/S0012-821X(01)00281-3.

Rawat, S., Gupta, A.K., Srivastava, P., Sangode, S.J., and Nainwal, H.C., 2015, A 13,000 year record of environmental magnetic variations in the lake and peat deposits from the Chandra valley, Lahaul: Implications to Holocene monsoonal variability in the NW Himalaya: Palaeogeography, Palaeoclimatology, Palaeoecology, v. 440, p. 116–127, https://doi.org/10.1016/j.palaeo.2015.08.044.

Ritter, J.B., Miller, J.R., Enzel, Y., and Wells, S.G., 1995, Reconciling the roles of tectonism and climate in Quaternary alluvial fan evolution: Geology, v. 23, no. 3, p. 245–248, https://doi.org/10.1130/0091-7613(1995)023<0245:RTROTA>2.3.CO;2.

Saha, S., Owen, L.A., Orr, E.N., and Caffee, M.W., 2018, Timing and nature of Holocene glacier advances at the northwestern end of the Himalayan-Tibetan orogen: Quaternary Science Reviews, v. 187, p. 177–202, https://doi.org/10.1016/j.quascirev.2018.03.009.

Saha, S., Owen, L.A., Orr, E.N., and Caffee, M.W., 2019, High-frequency Holocene glacier fluctuations in the Himalayan-Tibetan orogen: Quaternary Science Reviews, v. 220, p. 372–400, https://doi.org/10.1016/j.quascirev.2019.07.021.

Scherler, D., Bookhagen, B., and Strecker, M.R., 2014, Tectonic control on ^{10}Be-derived erosion rates in the Garhwal Himalaya, India: Journal of Geophysical Research–Earth Surface, v. 119, no. 2, p. 83–105, https://doi.org/10.1002/2013JF002955.

Scherler, D., Bookhagen, B., Wulf, H., Preusser, F., and Strecker, M.R., 2015, Increased late Pleistocene erosion rates during fluvial aggradation in the Garhwal Himalaya, northern India: Earth and Planetary Science Letters, v. 428, p. 255–266, https://doi.org/10.1016/j.epsl.2015.06.034.

Schlup, M., Carter, A., Cosca, M., and Steck, A., 2003, Exhumation history of eastern Ladakh revealed by ^{40}Ar/^{39}Ar and fission-track ages: The Indus River–Tso Morari transect, NW Himalayas: Journal of the Geological Society, v. 160, p. 385–399, https://doi.org/10.1144/0016-764902-084.

Searle, M., 1986, Structural evolution and sequence of thrusting in the High Himalayan, Tibetan-Tethys and Indus suture zones of Zanskar and

Ladakh, western Himalaya: Journal of Structural Geology, v. 8, no. 8, p. 923–936, https://doi.org/10.1016/0191-8141(86)90037-4.

Seong, Y.B., Owen, L.A., Bishop, M.P., Bush, A., Clendon, P., Copland, L., Finkel, R., Kamp, U., and Shroder, J.F., 2007, Quaternary glacial history of the Central Karakoram: Quaternary Science Reviews, v. 26, p. 3384–3405, https://doi.org/10.1016/j.quascirev.2007.09.015.

Sharma, M.C., and Owen, L.A., 1996, Quaternary glacial history of NW Garhwal, central Himalayas: Quaternary Science Reviews, v. 15, no. 4, p. 335–365, https://doi.org/10.1016/0277-3791(95)00061-5.

Sharma, P., Bourgeois, M., Elmore, D., Granger, D., Lipschutz, M.E., Ma, X., Miller, T., Mueller, K., Rickey, F., Simms, P., and Vogt, S., 2000, PRIME lab AMS performance, upgrades and research applications: Nuclear Instruments & Methods in Physics Research, Section B, Beam Interactions with Materials and Atoms, v. 172, p. 112–123, https://doi.org/10.1016/S0168-583X(00)00132-4.

Shi, Y., Yu, G., Liu, X., Li, B., and Yao, T., 2001, Reconstruction of the 30–40 ka BP enhanced Indian monsoon climate based on geological records from the Tibetan Plateau: Palaeogeography, Palaeoclimatology, Palaeoecology, v. 169, no. 1–2, p. 69–83, https://doi.org/10.1016/S0031-0182(01)00216-4.

Sinha, A., Cannariato, K.G., Stott, L.D., Li, H.C., You, C.F., Cheng, H., Edwards, R.L., and Singh, I.B., 2005, Variability of Southwest Indian summer monsoon precipitation during the Bølling-Allerød: Geology, v. 33, no. 10, p. 813–816, https://doi.org/10.1130/G21498.1.

Srivastava, D., 2012, Status Report on Gangotri Glacier: New Delhi, India, Science and Engineering Research Board, Department of Science and Technology, Himalayan Glaciology Technical Report 3, p. 21–25.

Srivastava, P., Tripathi, J.K., Islam, R., and Jaiswal, M.K., 2008, Fashion and phases of late Pleistocene aggradation and incision in the Alaknanda River Valley, western Himalaya, India: Quaternary Research, v. 70, no. 1, p. 68–80, https://doi.org/10.1016/j.yqres.2008.03.009.

Srivastava, P., Agnihotri, R., Sharma, D., Meena, N., Sundriyal, Y.P., Saxena, A., Bhushan, R., Sawlani, R., Banerji, U.S., Sharma, C., Bisht, P., Rana, N., and Jayangondaperumal, R., 2017, 8000-year monsoonal record from Himalaya revealing reinforcement of tropical and global climate systems since mid-Holocene: Scientific Reports, v. 7, 14515, https://doi.org/10.1038/s41598-017-15143-9.

Steck, A., Epard, J., Vannay, J., Hunziker, J., Girard, M., Morard, A., and Robyr, M., 1998, Geological transect across the Tso Morari and Spiti areas—The nappe structures of the Tethys Himalayas: Eclogae Geologicae Helvetiae, v. 91, p. 103–121.

Strahler, A.N., 1952, Hypsometric (area-altitude) analysis of erosional topography: Geological Society of America Bulletin, v. 63, no. 11, p. 1117–1142, https://doi.org/10.1130/0016-7606(1952)63[1117:HAAOET]2.0.CO;2.

Su, Z., and Shi, Y., 2002, Response of monsoonal temperate glaciers to global warming since the Little Ice Age: Quaternary International, v. 97–98, p. 123–131, https://doi.org/10.1016/S1040-6182(02)00057-5.

Thakur, V., Joshi, M., Sahoo, D., Suresh, N., Jayangondapermal, R., and Singh, A., 2014, Partitioning of convergence in Northwest Sub-Himalaya: Estimation of late Quaternary uplift and convergence rates across the Kangra reentrant, north India: International Journal of Earth Sciences, v. 103, p. 1037–1056, https://doi.org/10.1007/s00531-014-1016-7.

Thiede, R.C., Bookhagen, B., Arrowsmith, JR., Sobel, E.R., and Strecker, M.R., 2004, Climatic control on rapid exhumation along the Southern Himalayan front: Earth and Planetary Science Letters, v. 222, no. 3–4, p. 791–806, https://doi.org/10.1016/j.epsl.2004.03.015.

Thompson, L.O., Yao, T., Davis, M.E., Henderson, K.A., Mosley-Thompson, E., Lin, P.N., Beer, J., Synal, H.A., Cole-Dai, J., and Bolzan, J.F., 1997, Tropical climate instability: The last glacial cycle from a Qinghai-Tibetan ice core: Science, v. 276, no. 5320, p. 1821–1825, https://doi.org/10.1126/science.276.5320.1821.

Tofelde, S., Schildgen, T.F., Savi, S., Pingel, H., Wickert, A.D., Bookhagen, B., Wittmann, H., Alonso, R.N., Cottle, J., and Strecker, M.R., 2017, 100 kyr fluvial cut-and-fill terrace cycles since the Middle Pleistocene in the southern Central Andes, NW Argentina: Earth and Planetary Science Letters, v. 473, p. 141–153, https://doi.org/10.1016/j.epsl.2017.06.001.

Uppala, S.M., Kållberg, P.W., Simmons, A.J., Andrae, U., Bechtold, V.D., Fiorino, M., Gibson, J.K., Haseler, J., Hernandez, A., Kelly, G.A., and Li, X., 2005, The ERA-40 re-analysis: Quarterly Journal of the Royal Meteorological Society, v. 131, no. 612, p. 2961–3012, https://doi.org/10.1256/qj.04.176.

Vannay, C., Grasemann, B., Rahn, M., Frank, W., Carter, A., Baudraz, V., and Cosca, M., 2004, Miocene to Holocene exhumation of metamorphic crustal wedges in the NW Himalaya: Evidence for tectonic extrusion coupled to fluvial erosion: Tectonics, v. 23, TC1014, https://doi.org/10.1029/2002TC001429.

Wagnon, P., Linda, A., Arnaud, Y., Kumar, R., Sharma, P., Vincent, C., Pottakkal, J.G., Berthier, E., Ramanathan, A., Hasnain, S.I., and Chevallier, P., 2007, Four years of mass balance on Chhota Shigri Glacier, Himachal Pradesh, India, a new benchmark glacier in the western Himalaya: Journal of Glaciology, v. 53, no. 183, p. 603–611, https://doi.org/10.3189/002214307784409306.

Wang, Y., Cheng, H., Edwards, R.L., He, Y., Kong, X., An, Z., Wu, J., Kelly, M.J., Dykoski, C.A., and Li, X., 2005, The Holocene Asian Monsoon: Links to solar changes and North Atlantic climate: Science, v. 308, no. 5723, p. 854–857, https://doi.org/10.1126/science.1106296.

Watanabe, T., Dali, L., and Shiraiwa, T., 1998, Slope denudation and the supply of debris to cones in Langtang Himal, central Nepal Himalaya: Geomorphology, v. 26, no. 1–3, p. 185–197, https://doi.org/10.1016/S0169-555X(98)00058-0.

Wittmann, H., and Von Blanckenburg, F., 2009, Cosmogenic nuclide budgeting of floodplain sediment transfer: Geomorphology, v. 109, no. 3–4, p. 246–256, https://doi.org/10.1016/j.geomorph.2009.03.006.

Wulf, H., Bookhagen, B., and Scherler, D., 2010, Seasonal precipitation gradients and their impact on fluvial sediment flux in the Northwest Himalaya: Geomorphology, v. 118, no. 1–2, p. 13–21, https://doi.org/10.1016/j.geomorph.2009.12.003.

Wünnemann, B., Demske, D., Tarasov, P., Kotlia, B.S., Reinhardt, C., Bloemendal, J., Diekmann, B., Hartmann, K., Krois, J., Riedel, F., and Arya, N., 2010, Hydrological evolution during the last 15 kyr in the Tso Kar lake basin (Ladakh, India), derived from geomorphological, sedimentological and palynological records: Quaternary Science Reviews, v. 29, no. 9–10, p. 1138–1155, https://doi.org/10.1016/j.quascirev.2010.02.017.

Zehfuss, P.H., Bierman, P.R., Gillespie, A.R., Burke, R.M., and Caffee, M.W., 2001, Slip rates on the Fish Springs fault, Owens Valley, California, deduced from cosmogenic ^{10}Be and ^{26}Al and soil development on fan surfaces: Geological Society of America Bulletin, v. 113, no. 2, p. 241–255, https://doi.org/10.1130/0016-7606(2001)113<0241:SROTFS>2.0.CO;2.

Manuscript Accepted by the Society 23 December 2019

Printed in the USA